Pergamon

Geochimica et Cosmochimica Acta, Vol. 65, No. 9, pp. 1481–1498, 2001

0016-7037/01 $20.00 + .00

PII S0016-7037(01)00550-6

Trace element diffusion in andesitic melts: An application of synchrotron X-ray fluorescence analysis

J. KOEPKE* and H. BEHRENS

Institut für Mineralogie, Universität Hannover, Welfengarten 1, D-30167 Hannover, Germany

(*Received May* 19, 2000; *accepted in revised form December* 12, 2000)

Abstract—We have investigated the diffusivity of trace elements in hydrous iron-free andesitic melts containing 4.5 to 5.2 wt.% water at a pressure of 500 MPa and at temperatures between 1100 and 1400°C using the diffusion couple technique. The studied elements can be combined in several groups of particular geochemical interest: low field strength elements (LFSE: Rb, Sr, Ba), transition elements (Cr, Fe, Ni, Zn), rare earth elements (REE: La, Nd, Sm, Eu, Gd, Er, Yb, Y), and high field strength elements (HFSE: Zr, Nb, Hf). The diffusion profiles of the trace elements were measured using the synchrotron X-ray fluorescence (SYXRF) microprobe. H_2O distribution in the samples was analyzed by IR microspectroscopy.

Diffusion profiles are excellently reproduced, assuming concentration-independent diffusion coefficients. For all trace elements, the temperature dependence of diffusion in the hydrous melt can be described by a simple Arrhenius law. In general, the diffusivity decreases from the LFSE, to transition elements, to REE, and to the HFSE, a trend that can be correlated to the increase of charge in the same order. The activation energy shows a similar trend, increasing from 129 kJ/mol for Rb to 189 kJ/mol for Zr. For the transition elements Cr and Fe, the activation energy is relatively high (228 and 193 kJ/mol, respectively), which can be explained by increasing contributions of divalent cations to the diffusion flux with increasing temperature. Higher diffusivity of Eu compared to its neighbor elements also is attributed to contributions of divalent cations. Modeling Eu-diffusivity using data of Sr as representative for Eu^{2+}, and of Sm and Gd as representative for Eu^{3+}, shows that at all temperatures Eu^{3+} is clearly dominating in the hydrous melt. To quantify the effect of water, an additional experiment was performed at 1400°C using a nominally anhydrous melt. The obtained diffusion coefficients are (for most of the elements) by one and a half orders of magnitude lower than for a melt containing 4.5 wt.% H_2O.

Chemical diffusion coefficients D_η, which were calculated from the viscosity data of Richet et al. (1996) using the Eyring equation, and which assumed a jump distance of 3 Å, are in excellent agreement with the diffusivity of the HFSE for both dry and hydrous melt. Most of the investigated elements show a linear relation between log diffusivity and log viscosity, enabling the prediction of diffusivities in hydrous andesite systems at various conditions. Provided viscosity data are available, we suggest that this relation can be a useful tool to estimate trace element diffusivities for silicate melts with different compositions.

The new diffusion data show that water strongly enhances diffusivity of trace elements in andesitic melts. After 10,000 yr at 1200°C, diffusion produces in the dry melt relatively short profiles with lengths (defined as $x = (Dt)^{1/2}$) between 0.8 and 0.07 m (for Sr and Zr, respectively), whereas in hydrous melts (5 wt.% water), profiles are much longer with lengths between 3.9 and 0.92 m (for Sr and Zr, respectively).

1. INTRODUCTION

Diffusive transport in silicate melts is important in various magmatic processes. For example, chemical diffusion controls the growth and dissolution of crystals, the degree of contamination of magmas by xenoliths and wall-rocks, and the rate of chemical and isotopic homogenization during magma mixing. Results of previous studies on diffusion in silicate melts, as reviewed by Hofmann (1980) and Chakraborty (1995), suggest that diffusion in silicate melts is relatively slow, and that on a geologic time scale diffusion is unimportant in large-scale magma mixing. This statement, however, only is valid under static conditions with a planar interface of the magma bodies. A recent study by Snyder and Tait (1998) shows that in the case of a large surface area with a "fingered" flow morphology at the contact between basaltic and rhyolitic magmas, diffusion in the melt can be an important mixing process when combined with advection, at least for the mobile trace elements. These authors demonstrate that a basaltic magma can partly impart, on a large scale, its trace element and isotopic characteristics to a silicic magma by diffusion without significantly changing the major-element composition. According to the authors this can explain the trace element characteristics of the Bishop Tuff (California, USA). Other field and geochemical studies suggest that mobile trace elements can be redistributed during interaction at magmatic conditions, and that isotopic compositions can be modified selectively by diffusion (Grove et al., 1988; Baker, 1989; Lesher, 1990; Allen, 1991; Blichert-Toft et al., 1992).

For quantitative modeling of the behavior of trace elements in natural systems, there is a need for reliable tracer diffusion data for a great number of elements in silicate liquids of different compositions. Furthermore, because water is an abundant component in natural silicate melts (e.g., ~6 wt.% H_2O in the Pinatubo dacite magma; see review by Johnson et al., 1994), which significantly influences chemical and physical

*Author to whom correspondence should be addressed (koepke@mineralogie.uni-hannover.de).

properties of the melts (see reviews by Zhang, 1999 and Lange, 1994, and references therein), there is a need for a better understanding the mechanisms of diffusion in hydrous systems and for the collection of systematic element-specific diffusion data in hydrous silicate melts under pressure.

Diffusion of trace elements in dry silicate melts has been measured previously in numerous experimental studies performed at 1 atm and higher pressures (Hofmann, 1980; Jambon, 1982; Lowry et al., 1982; Baker, 1990, 1992; Baker and Watson, 1988; Lesher, 1994; LaTourette et al., 1996; Perez and Dunn, 1996; LaTourette and Wasserburg, 1997; Mungall and Dingwell, 1997; Nakamura and Kushiro, 1998; Mungall et al., 1999). However, diffusion data for hydrous silicate melts are rare. See reviews by Watson (1994) and Chakraborty (1995) and recent studies of Linnen et al. (1996), Mungall and Dingwell (1997), and Mungall et al. (1999).

Harrison and Watson (1983, 1984) and Rapp and Watson (1986) studied the diffusivities of Zr, Si, Ca, and P, and the light REEs, respectively, in hydrous granitic melts via the dissolution of zircon, apatite, and monazite. The results of these papers were summarized by Watson (1994): The addition of water to a silicate melt raises diffusion coefficients and lowers activation energies of diffusion, whereas elements with a low diffusivity in dry melts (e.g., Zr, P, Si) exhibit the greatest enhancement by adding water. Chekhmir and Epel'baum (1991) performed dissolution experiments in hydrous albitic melts and derived chemical diffusion coefficients for the main components of the system. Although the dissolution experiments have improved considerably our knowledge of the transport rates in wet silicate melt systems, this technique has several potential problems, which makes the collection of systematic trace element diffusion data difficult, i.e., moving mineral/melt interface (Chekhmir and Epel'baum, 1991) and coupling of diffusive fluxes.

The diffusion couple technique was applied only in a few experimental studies on tracer diffusion in hydrous silicate melts. A review of older studies is given by Watson (1994). Perez and Dunn (1996) measured the tracer diffusivity of Pb in a natural rhyolite melt at 0.1 GPa at nominally dry (~0.6 wt.% H_2O) and hydrous (~1 and ~2.5 wt.% H_2O) conditions. Unfortunately the water contents in the hydrous couples vary widely (0.88–1.61 and 2.26–3.52 wt.% H_2O, respectively) so that quantification of the relation between diffusivity and water content is difficult from these data. Mungall and Dingwell (1997) measured the diffusion of U and Th in melts of haplogranitic composition both in dry and hydrous systems, although they focused more on the dry system. According to these authors the transport of actinide is 2.5 orders of magnitude faster in granitic melt containing 5 wt.% water than in a dry melt. Due to variations of water content in the diffusion couples, it was not possible to determine an Arrhenius relation for the hydrous system. In a recent paper by Mungall et al. (1999), the diffusivities of 18 trace elements of different geochemical behavior in a nominally dry and in a hydrous (~3.7 wt.%) synthetic haplogranitic melt were investigated. This was the first successful attempt in collecting a great number of diffusion coefficients from a single experiment using an analytic method enabling multi-elemental data acquisition. Thus, the relative errors of the diffusion coefficients were minimized giving the potential to investigate systematic dependencies of the diffusivities on ionic charge and radius (an "internally consistent" data set, according to Mungall et al., 1999).

We report here results of an experimental investigation on trace element diffusion in hydrous andesitic melts at 500 MPa using the diffusion coupling technique. The selected elements belong to four groups of particular geochemical interest: low field strength elements (LFSE), rare earth elements (REE), high field strength elements (HFSE), and transition elements. The purpose of this paper is (1) to present internally consistent diffusion data for hydrous andesitic melts, (2) to quantify the difference between hydrous (5 wt.% H_2O) and nominally dry melts, (3) to investigate small but systematic variations within one element group (e.g., REE) using a high precision analytic technique, and (4) to gain new insights into the mechanisms controlling the transport of trace elements in silicate melts.

As the main analytic instrument we used SYXRF (synchrotron X-ray fluorescence) microprobe, which is well suited for the analysis of multi-elemental trace element concentration profiles in silicate systems. Baker (1989, 1990) and Baker and Watson (1988) successfully applied the SYXRF microprobe to measure trace element profiles in rhyolite/dacite diffusion couples. Since those studies to our knowledge, the SYXRF microprobe was never used for similar analytic problems, although it offers some interesting advantages as shown in this paper.

2. EXPERIMENTAL AND ANALYTIC METHODS

2.1. Starting Material

Natural andesite contains high concentrations of iron, which can cause several experimental and analytic problems. Dissolution of iron in the capsule walls and changes of the redox state of iron during the experiments, if the melts are not preequilibrated at same conditions, can produce time-dependent effects that interfere with the diffusion of trace elements. Further, a very large concentration of iron decreases the spectral resolution of the fluorescence lines of the neighboring elements.

To avoid these problems, we used an iron-free andesite, substituting FeO by equimolar portions of CaO and MgO, and Fe_2O_3 by Al_2O_3, so that the NBO/T (number of non-bridging oxygen/number of tetrahedral cations) correspond to the iron-bearing system. Since the role of Fe^{2+} in silicate melts with respect to its behavior as network former or modifier is still under debate (e.g., Rossano et al., 2000), this procedure could only be regarded as an approach to realistic conditions.

The basic (iron-bearing) composition was derived from glasses produced by dehydration melting of synthetic amphibolite in our lab. The Fe_2O_3/FeO ratio of the melt at experimental conditions was estimated after Kilinc et al. (1983), assuming an oxygen fugacity of NNO +3 and a temperature of 1200°C. A glass with the calculated composition was produced by fusion of a mixture of oxides and carbonates in a platinum crucible at 1600°C. The composition of the glass (Table 1) is similar to that of the iron-free analog of an andesite from Montagne Pelée, which was used by Richet et al. (1996) in a viscosity study. As shown by these authors, the viscosity of the iron-free analog is close to that of the natural, iron bearing melt, at least for dry melts.

A part of the glass was doped for the diffusion experiments with 300 ppm of various trace elements: LFSE (Rb, Sr, Ba), REE (La, Nd, Sm, Eu, Gd, Er, Yb, Y), HFSE (Ti, Zr, Nb, Hf, Ta) and transition elements (Sc, Cr, Fe, Ni, Zn). To insure homogeneous trace element distribution, predried oxides and carbonates were mixed intensively with glass powder in a ball mill for 8 h before melting at 1600°C.

Dry cylinders were produced by melting predried glass powder in sealed platinum capsules at ambient pressure at 1600°C for 5 h. To produce large hydrous glasses of cylindrical shape, dry glasses were crushed in a steel mortar and sieved to fractions with grains sizes of 200 to 500 μm and $<$200 μm. To minimize the pore volume of the powder, the two fractions were mixed in weight ratio of 1:1. The mixture was

Table 1. Chemical composition of the undoped starting glasses.

Glass	SiO_2	Al_2O_3	MgO	CaO	Na_2O	K_2O	Total	H_2O
Hydrous	62.09	19.47	2.53	10.64	4.25	1.02	100.00	4.92
sd	0.37	0.42	0.03	0.15	0.18	0.06		
Nominal dry	61.81	19.48	2.51	10.82	4.30	1.03	99.95	
sd	0.12	0.24	0.06	0.09	0.20	0.06		

Concentrations were measured by electron microprobe; sd refers to the standard deviation of each set of 7 points. For comparison, the analysis of the hydrous glass is normalized to 100 wt.%. The water concentration of the hydrous glass was measured by Karl-Fischer titration (average of 2 analyses of small pieces from both ends of the glass cylinders).

inserted into Pt capsules (35 mm long, 4 mm diameter, 0.2 mm wall thickness) and stuffed intensively with the help of a steel piston. Added to the capsule was 5 wt.% of doubly distilled water in four steps to achieve a homogeneous water distribution within the cylinders. The sealed capsules were heated in an internally heated pressure vessel (IHPV) at 1200°C, 500 MPa for 4 d.

The compositions of the synthesized glasses were checked by electron microprobe for homogeneity with respect to the major elements (Si, Al, Mg, Ca, Na, K). The concentrations of the trace elements in the glasses were checked by XRF and ICP-MS (inductively coupled plasma-mass spectrometry) analysis. The water contents of the hydrous glasses were determined by Karl-Fischer titration (Behrens, 1995). The homogeneity of the water distribution in the glasses was checked by analyzing two small pieces (10–20 mg) from both ends of the glass cylinders. The measured water concentrations varied from 4.80 to 5.06 wt.%.

For the diffusion experiments the synthesized glass cylinders were cut into small pieces (~3 mm long) and polished on one side. Diffusion couples were prepared by aligning a trace element free cylinder and a doped cylinder in a platinum capsule with the polished sides in contact. Capsules were sealed to prevent loss of water during the experiments.

2.2. Experimental Techniques

Experiments were performed in a vertically operating IHPV pressurized with argon. Pressure was measured with a strain gauge manometer with an uncertainty of ± 50 bar. To minimize the heating-up and the cooling-down periods of the experiments, a furnace with three independent heating loops was designed. An outer furnace, which consists of two Mo wire heating loops (upper and lower loop), was used to heat the sample with a ramp of 30°C/min to a temperature of ~800°C. Then a constant power was manually adjusted at both loops to hold the temperature. The outer furnace served only as a heating pool. Rapid heating (100°C/min) to the run temperature was achieved by inserting an additional small tube furnace into the outer furnace, which contained the sample holder. This high T furnace, which was used up to 1400°C, consists of a small corundum tube (12 mm outer diameter, 8 mm inner diameter) with one Mo winding over 40 mm long. Temperature was measured with three or four S-type thermocouples over a distance of 30 mm. Variations in T over the sample was less than 10°C in all experiments, and temperature is believed to be accurate within ±10°C. After the run, the samples were quenched isobarically by turning off the power to the furnace. Because of the small mass of the inner loop containing the sample, initial quenching rates on the order of 400°C/min were reached. The effect of heating-up and cooling-down on the tracer diffusivities was tested by a zero-time experiment at 1100°C, in which the diffusion sample was quenched immediately after reaching the run temperature.

Conditions in the IHPV are relatively oxidizing. Using NiPd sensors, oxygen fugacities of NNO (Ni/NiO oxygen buffer) + 2.3 at 850°C, 500 Mpa, and NNO + 3.5 at 1100°C, 500 Mpa, were determined by Wilke and Behrens (1999) and Tamic et al. (2000), respectively, for water saturated conditions. In our experiments, melts always are water-undersaturated so that the oxygen fugacity is lower. At experimental conditions, transport of water and hydrogen in silicate melts (H_2O diffusion, e.g., Behrens and Nowak, 1997, Zhang and Behrens, 2000, H_2 diffusion, e.g., Chekmir et al., 1985; Schmidt, 1996; Gaillard et al., 1998) and permeation of hydrogen through the Pt capsule (Chou, 1986) are fast compared to cation diffusion. Rough calculations suggest that the redox conditions in the diffusion sample are established within a few minutes. Thus, the effect of changing the oxygen fugacity during the experiments, which would influence the diffusion of polyvalent cations, can be neglected.

2.3. The Synchrotron X-ray Fluorescence Microprobe (SYXRF)

After the runs, the capsules were cut perpendicular to the contact plane of the couple and doubly polished thin sections were prepared for microanalytic measurements. In all experiments the original contact plane was visible by a small offset in the alignment of the starting glass cylinders.

The diffusion profiles of the trace elements were measured using the SYXRF microprobe of the HASYLAB at DESY (Deutsches Elektronen-Synchrotron, Hamburg, Germany). A schematic drawing of the X-ray microprobe installed at beamline "L" at the DORIS III synchrotron source is shown in Figure 1. The method is well established for the local analysis of trace elements in the earth sciences, as seen in detailed reviews by Smith and Rivers (1995) and Haller and Knöchel (1996), and offers a number of interesting advantages in comparison with other microanalysis techniques: (1) collection of multi-element spectra with one acquisition only, (2) practically damage-free analysis enabling long-time acquisition under steady-state conditions, (3) negligible matrix effects due to water in the glasses, which contrasts with matrix effects observed in SIMS analysis of hydrous glasses (Koepke et al., 1998), and (4) easy analysis and quantification of the X-ray spectra, enabling automatic processing of a great number of X-ray spectra within a short time (more than 1000 in this study). For our measurements we used the "white" X-ray continuum of the DORIS III bending magnet with an energy maximum at 16.5 keV (critical energy), pro-

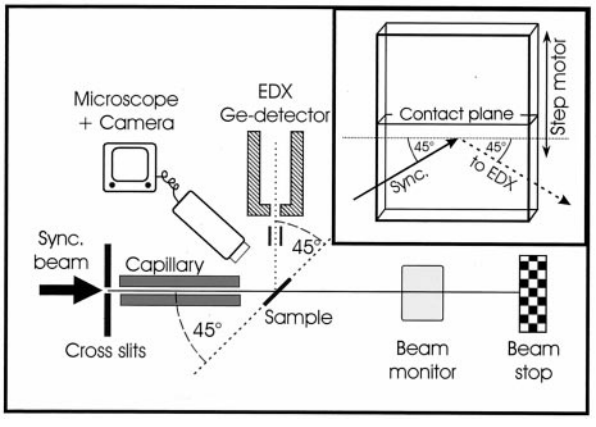

Fig. 1. Schematic drawing of the SYXRF spectrometer installed at beamline L at HASYLAB (top view). The inset shows a view of the sample orientation (see text for details). For the acquisition of concentration profiles a step motor moves the sample perpendicular to the contact plane of the diffusion couple.

viding radiation intensities sufficiently high to excite K-shell fluorescence up to 80 keV. This means that even heavy elements, e.g., Pb, can be identified by their K-radiation. In our study we have measured simultaneously the K-spectra of 21 trace elements with the help of an energy-dispersive Ge semiconductor. To minimize Rayleigh and Compton scattering, we used the so-called "horizontal" geometry (Haller and Knöchel, 1996), in which the angle of incidence of the synchrotron beam on the sample is 45° and the fluorescence radiation is detected at a scattering angle of 90° (Fig. 1).

Glass capillaries were used to reduce the diameter of the incoming beam. In most of the diffusion couples the length of the concentration profiles varied between 1 and 6 mm, and a sufficient local resolution could be achieved with a capillary of 20 μm inner diameter. A focusing capillary providing a better resolution (3 μm diameter) was used only for the zero-time run in which the diffusion profiles are very short. The disadvantage of this type of capillary is the large reduction of the X-ray intensities at high energy, lowering the precision of data acquisition (Haller et al., 1995). Therefore, we did not used it for routine measurements. Because the synchrotron radiation passes through the sample without significant absorption, a cylinder-like volume is analyzed and the local resolution depends strongly on sample thickness and orientation. This contrasts with other microanalytic tools for trace elements like SIMS or LA-ICP-MS (laser ablation inductively coupled plasma-mass spectrometry), which produce crater-like spots only at the surfaces of the samples. However, this disadvantage of SYXRF can be overcome in diffusion studies by using very thin samples (30–50 μm) and aligning the contact plane of the diffusion couple parallel to the plane of the incoming beam and the direction of detection (Fig. 1). Thus, a resolution similar to the diameter of the capillary can be achieved. Excellent spectra could be obtained with a relatively short acquisition time of 4 min. Peak fitting and determination of the net peak areas were done with the help of commercial software, AXIL (van Espen et al., 1977). The net intensities were normalized to an internal standard (Ca) to eliminate fluctuations of the synchrotron beam and to cancel out effects due to the thickness of the sample. These intensity ratios are proportional to the concentration of the trace element in the glass. No matrix correction with respect to the main elements was necessary because the main element compositions of the doped and the undoped glasses are identical (only 0.6 wt.% of trace element oxides were added in total). The sensitivity of the method depends strongly on the intensity of the synchrotron source, which is low at high energies (K-shell radiation of, for example, Yb and Hf) and high at the medium energies (K-shell radiation of, for example, Sr and Zr). In addition, the sensitivity is reduced at low energy by absorption of soft X-rays by air. Reliable measurements were possible for Ca and elements with higher atomic numbers. However, in the case of Sc and Ti, which have a relatively low K-shell energy, the concentrations in our samples were not high enough to resolve the fluorescence peaks accurately. No reliable measurements were possible with Ta because its weak signal is close to the high energy limit of the synchrotron source, and it is affected by the high background radiation from Ta used in the cross slit system. The analytic reproducibility obtained for the homogeneous doped glass (300 ppm) varies from ~1% for elements like Sr to ~10% for elements like Yb. It is worth mentioning that the analysis of the REE by SYXRF is not hampered by overlapping K-lines. This contrasts with SIMS, where measurements of some REE in multi-element doped silicate glasses is problematic due to isobaric interferences as stated by Nakamura and Kushiro (1998).

2.4. Other Analytic Methods

Main elements (Si, Al, Mg, Ca, Na, K) were analysed using a Cameca Camebax electron microprobe equipped with a SAMX operating system. All data were obtained using 15 kV acceleration potential, a fixed, defocused beam with a spot size of 10 to 20 μm, a current of 18 nA, 2 s counting time for Na and K and 5 s for the other elements, and a matrix correction according to the "PAP method" of Pouchou and Pichoir (1991). Under these conditions no migration or volatilization of sodium or potassium was observed. All samples were carefully checked with backscattered electron images for bubbles or crystals.

Water content along the diffusion profiles was analyzed by IR microspectroscopy. Spectra were recorded in the mid-infrared using an

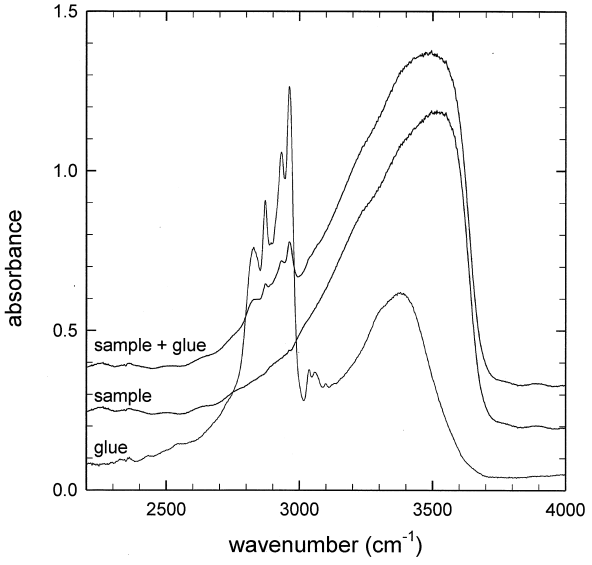

Fig. 2. IR spectroscopy on diffusion sample JK60 at the interface. The measured spectrum is a composite of the spectrum of the sample and the glue (Araldit). The sample spectra was obtained after subtracting spectrum of the glue scaled to same intensity of the baseline-corrected peak at 2962 cm^{-1}. Effective thickness of the sample is 22 μm.

A590 IR microscope attached to a Bruker IFS88 FTIR spectrometer. Measurement conditions were halogen light source, KBr beamsplitter, and HgCdTe detector. Typically, 50 to 100 scans were accumulated for each spectrum with a spectral resolution of 2 cm^{-1}. The analyzed volume was limited to a width of ~30 μm using a slit aperture adjusted between objective and detector.

A linear baseline was fitted to the spectra in the range 4100 to 4800 cm^{-1} and was subtracted from the spectra. Total water concentrations were determined from the baseline-corrected peak height of the absorption band at 3530 cm^{-1}, using the Lambert-Beer law. In the evaluation we have used a density to water content relationship (density [in g/L] = 2518 − 15.2 · c_{H2O}, with concentration of H_2O in wt.%) based on data for a similar andesitic composition (Richet et al. 1996), and an experimentally determined linear molar absorption coefficient for the band (66 L/mol_{H2O} cm, based on two samples containing 4.92 and 4.84 wt.% H_2O).

In general, the sections of hydrous glasses used for SYXRF were too thick for IR measure and had to be thinned to <30 μm. The preparation of free thin sections with length >6 mm is extremely difficult because of bending and breaking. Therefore, for polishing we fixed the sections with a thin layer of epoxy (Araldit) on polished plates of an extremely water-poor silica glass (Infrasil, <5 ppm H_2O). Background spectra were recorded on the Infrasil glass and thus the sample spectrum only contained contributions from the glass and from the epoxy. To remove the contribution of epoxy, a spectrum of pure Araldit scaled by the height of the most intensive band at 2962 cm^{-1} was subtracted from the sample spectrum (Fig. 2). The maximum of the OH vibration band is at lower wavenumber for the epoxy (3380 cm^{-1}) than for the glass (3530 cm^{-1}), and the intensity in the epoxy spectrum is relatively small at the OH peak maximum of the glass (15% of the absorbance at 2962 cm^{-1}). Thus, the intensity of the OH peak in the glass can be determined precisely (±2% relative) if the band at 2962 cm^{-1} is significantly smaller than the total OH peak.

The thickness of glass wafers was determined from interference fringes in the sample spectra. The distance between the maxima of the interference fringes ($\Delta\nu$) is inversely proportional to the thickness of glass + epoxy layer (d_{s+e}). Using 5 andesitic samples ranging from 37 to 61 μm, we obtained the relation to be $d_{s+e} = 0.319/\Delta\nu$. The coefficient in this equation is nearly identical (0.3176) to that determined by Tamic et al. (2000) for free sections of rhyolitic glasses. This

indicates that the method for thickness determination is not very sensitive to the composition. On the other hand, the coefficient is expected to be dependent on the beam path through sample and thus, on the type of IR microscope. To get the sample thickness, the thickness of the epoxy layer must be known. This value was measured by the intensity of the 2963 cm^{-1} band in the Araldit spectrum subtracted from the sample spectrum using an experimentally determined absorbance/thickness ratio of 0.0605/μm.

Based on the reproducibility of IR measurements, and on agreement between bulk analysis of water by Karl-Fischer titration (KFT) and local analysis by IR, we estimate the uncertainty of IR measurements to be 0.2 wt.% for the hydrous samples. The precision is higher for the nominally anhydrous glass because a thicker section (1 mm) could be analyzed. However, the absorption coefficient was not calibrated at such low water contents and may have an unknown error if applied to water-poor glasses.

3. RESULTS

All diffusion experiments with hydrous glasses in the range 1100 to 1400°C provide crystal-free and bubble-free glasses, indicating superliquidus conditions. With the anhydrous composition, only one run at 1400°C was successful. At lower temperatures up to 1310°C, anhydrous samples were partially crystallized. These observations demonstrate the strong depressing effect of H_2O on the liquidus in the iron-free andesitic system. At 500 Mpa, the anhydrous liquidus is at least 210°C higher than the liquidus with 5 wt.% H_2O.

Diffusion experiments with hydrous melts might be complicated by local and temporary variation in H_2O concentration due to (1) initial difference in water content of the two halves (up to 0.3 wt.% in our samples) and (2) small amounts of air enclosed in the capsule by preparation. Condition (1) produces an H_2O flux parallel to the direction of cation diffusion. In the case of condition (2), a water-undersaturated fluid phase is present at least at the beginning of the experiment, and H_2O fluxes can occur parallel or perpendicular to the cation fluxes, depending on the location of the fluid in the capsule. Both effects seem to be minor in our experiments. H_2O concentration gradients were not observed in any of the experiments (see Table 2), and the water contents measured by IR after the experiments usually are close to the initial water contents. An exception is sample JK63, which had a relatively low water content after the run (4.5 wt.%). We suggest that this particular sample was partially dehydrated during the run due to entrapped air. However, we made no attempt to identify a free fluid phase, for instance, by piercing and drying the capsule after the run, because this may result in water loss from the glass. Thus, we cannot prove dehydration in the experiments.

The absence of H_2O gradients in the glasses is consistent with water diffusion data for silicate melts. Based on data for granitic melts (Nowak and Behrens, 1997; Mungall et al., 1998; Zhang and Behrens, 2000) and basaltic melts (Zhang and Stolper, 1991), we estimate the bulk water diffusivity for andesitic melt containing 5 wt.% H_2O to be on the order of 1×10^{-10} m^2/s at 1200°C, similar to the diffusivity of the mobile cations Rb and Sr. Any H_2O concentration gradient present at the beginning of the experiment (e.g., at the contact of the halves) will be rapidly smeared out. Further support that water fluxes should not have affected the diffusion of trace elements is given by Mungall et al. (1998).

3.1. Evaluation of Diffusion Profiles

Assuming a concentration-independent diffusion coefficient, the solution of Ficks' second law for the given boundary conditions (semi-infinite medium, concentration step at the beginning, concentration c_0 and c_1 in both halves of the diffusion couple) is:

$$(c - c_0)/(c_1 - c_0) = 0.5 \cdot (1 - \mathrm{erf}((x - a)/2(Dt)^{1/2})) \quad (1)$$

where c is the concentration at distance x, a is the position of the inflection point of the profile, t is the duration and D the diffusion coefficient.

Diffusion coefficients were determined by fitting the experimental concentration distance profiles to Eqn. 1. The zero point of the x-axis was arbitrarily chosen and thus the inflection point of the profile was an adjustable parameter of the fit. All the diffusion profiles referred to in Table 2 are fitted excellently by the diffusion equation.

Strictly speaking, the diffusion coefficients measured by our method are *chemical diffusion coefficients* of melt components, because diffusion is driven by imposed gradients of the chemical potentials of the components. The chemical diffusion coefficient can be expressed by $D_i^* * \phi$, where D_i^* is the self-diffusion coefficient and ϕ the thermodynamic factor. Whether the measured coefficients are indeed tracer diffusivities depends on the magnitude of the thermodynamic term (see discussion in Chakraborty 1995). Even for dilute components, this is not necessarily close to unity in all cases for silicate melts, as shown for example by the study of Lesher (1994) on Nd and Sr. However, the total concentration of trace elements in our study is very small (~0.6 wt.%) and both network former and modifier were added so that the NBO/T value is almost unchanged along the profiles. Thus, we infer that transport conditions are determined basically by the bulk composition of the melt and therefore, the diffusion coefficients can be considered as *tracer diffusion coefficients* (tracer diffusivity results from the random walk of individual ions in the absence of gradients in chemical potentials).

3.2. Convection or Diffusion?

Contributions of convection to the transport in melt can be a large problem in diffusion experiments, especially in low viscosity melts (e.g., Hofmann and Magaritz, 1977). There are several pieces of evidence that non-diffusive transport is not significant in our experiments:

1. In a zero-time experiment, the sample was heated to 1100°C and then immediately quenched. Assuming Arrhenius behavior of diffusion in the whole temperature range, effective durations at 1100°C were calculated for each element from the recorded time-temperature data using the individual activation energies given in Table 3. The effective time t_{eff} at temperature T_1 is:

$$t_{eff} = \int D_{T(t)}/D_{T1}\, dt = \int \exp(-E_a/R \cdot (1/T(t) - 1/T_1))\, dt \quad (2)$$

(see Zhang and Behrens, 2000). Calculated values of t_{eff} vary between 364 s for the fast Rb^+ and 241 s for the slow Zr^{4+}. In Figure 3 we compare the concentration distances profiles normalized by $t^{1/2}$ from the zero-time run with a long term-run

Table 2. Trace element diffusion data for andesitic melts.

No.		JKD3		JK60		JK61		HB72	JK63	JK67	
T (°C)		1100		1100		1200		1310	1400	1400	
t_{dwell} (s)		0		10800		7200		3600	1800	10800	
$t_{heat/cool}$ (s)[a]		[a]		217-366		245-415		76-144	89-162	–	
H_2O(wt%)[b]		5.0/**5.2**/5.2		4.9/**4.9**/5.1		5.0/**5.2**/5.0		5.1 [c]	4.3/**4.5**/4.7	0.058/**0.060**/0.064	
Position of profile		Center		Center 1st profile	Center 2nd profile	Center	Rim	Center	Center	Center	Rim
charge	z/r_{M-O}^2 [d] ($Å^{-2}$)	t_{eff} [a] (s)		D ($x10^{-12}$ m^2/s)							
Rb 1+	0.113 (VIII)	364	50	33.8 ± 7.3	32.9 ± 7.1	65.8 ± 13.5	64.4 ± 13.2	149 ± 29	251 ± 47	9.4 ± 1.8	8.5 ± 1.6
Sb 2+	0.291 (VIII)	314	34	22.3 ± 5.0	22.0 ± 4.9	48.5 ± 10.2	49.1 ± 10.3	122 ± 24	178 ± 34	12.9 ± 2.5	12.4 ± 2.4
Ba 2+	0.259 (VIII)	304	21	15.8 ± 4.8	14.5 ± 4.4	31.7 ± 9.2	36.1 ± 10.5	80.0 ± 22.4	133 ± 36	5.8 ± 1.6	5.1 ± 1.4
Cr (2+); 3+	0.773 (VI)	–	–	2.3 ± 0.9	2.1 ± 0.8	7.1 ± 2.5	7.4 ± 2.6	43.7 ± 14.7	62.6 ± 20.3	8.6 ± 2.8	10.3 ± 3.3
Fe 2+; 3+	-	–	–	7.9 ± 2.3	9.3 ± 2.7	18.1 ± 5.2	19.8 ± 5.6	91.6 ± 22.9	–	–	–
Ni 2+	0.476 (VI)	–	–	–	4.2 ± 1.4	8.5 ± 2.8	9.4 ± 3.1	34.6 ± 10.9	66.3 ± 20.1	–	–
Zn 2+	0.454 (VI)	–	–	10.1 ± 3.3	11.5 ± 3.8	21.1 ± 6.6	41.6 ± 13.0	72.0 ± 21.6	124 ± 36	–	6.5 ± 1.9
Y 3+	0.532 (VIII)	255	5.6	2.9 ± 0.7	2.9 ± 0.7	7.8 ± 1.9	7.7 ± 1.9	21.6 ± 4.9	44.6 ± 9.7	1.61 ± 0.35	1.31 ± 0.29
La 3+	0.465 (VIII)	261	9.4	4.0 ± 1.3	3.7 ± 1.2	10.3 ± 3.2	9.1 ± 2.8	27.2 ± 8.0	55.2 ± 15.8	2.1 ± 0.6	1.55 ± 0.44
Nd 3+	0.488 (VIII)	261	8.5	4.3 ± 1.4	3.9 ± 1.3	10.3 ± 3.2	12.5 ± 3.9	29.3 ± 8.6	58.1 ± 16.6	2.1 ± 0.6	2.7 ± 0.8
Sm 3+	0.500 (VIII)	255	8.0	3.6 ± 1.2	3.3 ± 1.1	8.9 ± 2.8	8.7 ± 2.7	26.1 ± 7.8	53.6 ± 15.5	1.79 ± 0.52	1.52 ± 0.44
Eu 2+; 3+	-	267	13.0	4.2 ± 1.3	4.1 ± 1.3	11.6 ± 3.6	13.5 ± 4.1	32.9 ± 9.6	51.6 ± 14.7	5.3 ± 1.5	7.6 ± 2.2
Gd 3+	0.512 (VIII)	267	5.3	3.6 ± 1.2	3.2 ± 1.0	8.9 ± 2.7	7.0 ± 2.1	21.6 ± 6.3	45.0 ± 12.7	1.43 ± 0.41	–
Er 3+	0.539 (VIII)	273	5.3	4.0 ± 2.1	2.5 ± 1.3	9.8 ± 5.0	10.2 ± 5.2	18.1 ± 9.0	36.5 ± 17.8	1.50 ± 0.73	–
Yb 3+	0.603 (VIII)	–	–	–	2.6 ± 1.4	10.2 ± 5.4	–	19.1 ± 9.8	52.0 ± 26.1	–	–
Zr 4+	0.925 (VI)	241	2.0	0.92 ± 0.27	0.90 ± 0.26	2.7 ± 0.7	2.7 ± 0.7	8.3 ± 2.1	17.4 ± 4.3	0.53 ± 0.13	0.46 ± 0.11
Nb (3+); 5+	1.250 (VI)	255	3.3	1.59 ± 0.44	1.51 ± 0.42	4.3 ± 1.1	4.2 ± 1.1	11.6 ± 2.9	23.9 ± 55.7	0.78 ± 0.19	0.71 ± 0.17
Hf 4+	0.934 (VI)	252	4.7	1.09 ± 0.60	0.83 ± 0.46	3.8 ± 2.0	–	7.8 ± 4.1	15.1 ± 7.7	–	–
Chemical diffusion[c]				0.90		3.4		11.6	27.3	0.47	

[a] Effective run durations (t_{eff}) in the zero-time experiment and contributions of heating and cooling to the effective duration of the other experiments ($t_{heat/cool}$) were calculated individually for each cation using the activation energies summarized in Table 3.

[b] The reported values of total water are measured at the contact plane of the two halves of the diffusion couple (in bold) and at 1 mm distance to the contact on both sides.

[c] For sample HB72 the given value corresponds to the average of three measures close to the rim of the sample.

[d] The ionic field strength z/r_{M-O}^2 of monovalent cations and cations for which one oxidation state is clearly dominating was calculated using cation radii and the radius of 3-coordinated oxygen (1.36Å) from Shannon (1976) and the charge z from column 2. Assumed coordination is given in parenthesis.

[e] Chemical diffusivity was calculated from viscosity data of Richet et al. (1996) by the Eyring equation assuming a jump distance of 3 Å (see text for details). Erros of the diffusion coefficients refer to the accuracy of the data.

held at 1100°C. If transport is controlled by diffusion, the profiles should be identical. In fact, considering the large difference in effective run duration, the agreement of the profiles is excellent. The obtained diffusion coefficients are only higher by factor of two in the zero-time experiment for all elements except Eu. The slightly higher values in the zero-time run may be explained by a small contribution of non-diffusive transport during heating (as suggested for water diffusion in haplogranitic melts by Nowak and Behrens, 1997) and by the uncertainty in calculation of t_{eff}. The relatively large difference in the case of Eu may be explained by more reducing conditions at the beginning of the experiment.

2. Convection is expected to produce perturbations in the sample resulting in deviation of the profiles from error function shape and/or in a dependence of the inflection point of the profile from the distance to the axis of the couple. Profiles measured in the center of hydrous sample JK61 and anhydrous sample JK67 do not differ from profiles measured close to the rim, and as mentioned above, all profiles are excellently fitted by Eqn. 1, supporting negligible influence of convection.

3. In each experiment, large variations of diffusion coefficients are observed (e.g., by a factor of 40 at 1100°C), and the diffusion data are excellently described by an Arrhenius dependence (see below). Convection will average the transport rates of the cations. In fact, such averaging was observed in an experiment with the hydrous melt at 1300°C, which failed because a large bubble migrated through the melt during the run and produced non-diffusive mixing. The measured concentration profiles of this particular sample exhibit clear deviation from error function shape, and diffusion coefficients of less-mobile elements such as Zr and Nb are apparently increased when compared to other data in the Arrhenius plot.

3.3. Uncertainty of the Diffusion Data

Due to simultaneous measurement of all trace elements, the ratio between diffusion coefficients can be obtained with very high precision. The precision of our analytic method is determined mainly by the scatter of data points along a profile, which decreases with increasing intensity of the fluorescence signal of the element. Based on duplicated profiles in samples JK60, JK61, and JK67, the elements can be divided into three groups:

Table 3. Arrhenius parameters for trace element diffusion in hydrous andesitic melts (4.5–5.2 wt.% H_2O).

	Number of profiles used for regression	log D_0 (m^2/s)	E_a (kJ/mol)
Rb	6	−5.58 ± 0.14	129.1 ± 4.0
Sr	6	−5.44 ± 0.18	137.0 ± 5.0
Ba	6	−5.51 ± 0.16	139.8 ± 4.4
Cr	6	−3.00 ± 0.59	228 ± 17
Fe	5	−3.78 ± 0.99	193 ± 27
Ni	6	−4.39 ± 0.56	186 ± 16
Zn	6	−4.96 ± 0.40	159 ± 11
Y	6	−4.92 ± 0.07	174.2 ± 1.9
La	6	−4.99 ± 0.18	169.1 ± 5.1
Nd	6	−4.96 + 0.20	168.9 ± 5.5
Sm	6	−4.81 ± 0.17	175.2 ± 4.9
Eu	6	−5.06 ± 0.30	165.6 ± 8.4
Gd	6	−5.27 ± 0.31	163.5 ± 8.6
Er	6	−5.66 ± 0.53	152 ± 15
Yd	4	−4.66 ± 0.62	181 ± 18
Zr	6	−4.87 ± 0.06	188.7 ± 1.6
Nb	6	−5.19 ± 0.07	174.1 ± 2.0
Hf	5	−5.28 ± 0.51	176 ± 14

(1) high reproducibility (within 3 to 5%): Rb, Sr, Y, Zr, Nb,
(2) intermediate reproducibility (within 10 to 15%): Ba, Cr, Fe, Ni, Zn, La, Nd, Sm, Eu, Gd, and
(3) low reproducibility (within 30 to 50%): Yb, Er, Hf.

In addition, the precision of the diffusion coefficients is influenced by the uncertainty in temperature (10°C), effective run duration (~100 s) and water content (0.2 wt.% for hydrous samples). On the other hand, uncertainty of pressure (500 MPa) is expected to have no significant influence on transport properties of the melt. Kushiro (1976) shows that the pressure dependence of viscosity of dry andesitic melt is small with a variation of only 0.4 log units between 1 bar and 1.5 GPa. Results of White and Montana (1990) on feldspathic melts and Schulze et al. (1996) on haplogranitic melts indicate that the effect of pressure may be even smaller in the hydrous melt.

Errors due to the uncertainty of temperature on diffusivity ranges from 5 to 13%. For example, at 1400°C for the fast Rb, the propagated error in diffusivity is 5%, and for the slow Zr at 1100°C, the error is 13%. The errors due to the uncertainty in run duration vary between 1% at 1100°C and 4% at 1400°C. The possible errors due to uncertainty in the determination of the water content can be estimated from calculated viscosities (after Richet et al., 1996; for clarity see section 4.4) via the Eyring equation and range from 8% at 1100°C to 5% at 1400°C for the hydrous samples. Errors for the anhydrous melt could not be determined as rigorously, but are assumed to be similar to those for the hydrous melt. Based on these error estimates, we have calculated individually the uncertainty of the diffusion coefficients, which varies from 20% for high quality elements like Rb and Sr to around 50% for low quality elements such as Er, Yb, and Hf.

3.4. Diffusion of Transition Elements

In contrast to the other elements, the transition elements (especially Fe and Cr) are highly soluble in platinum under intrinsic conditions of the IHPV. Thus, the profiles of these elements may be affected by diffusion to the capsule walls. In fact, a decrease of concentration close to the end of the doped half is evident for Fe and Ni at 1100 and 1200°C (Fig. 4). However, the profiles of Cr, Fe, Ni, and Zn evolved between the halves of the diffusion couple always are shorter than the diameter of the cylinder (4 mm) and, therefore, we do not expect that the center of the couple is affected by diffusion to the walls. At 1200°C, profiles along the axis and close to the rim of the cylinder yield similar diffusivities for transition metals, supporting the contention that diffusion to the walls is of minor importance in our experiments.

3.5. Comparison of Tracer Diffusivities and Effect of Temperature

Diffusion data are summarized in Table 2. Although there are small differences in water content, the diffusion data of the trace elements for the hydrous melt can be described by a simple Arrhenius law:

$$D = D_0 \exp(-E_a/RT) \quad (3)$$

where D_0 is the preexponential factor and E_a the activation energy of diffusion. Arrhenius plots of selected elements of each group are shown in Figure 5. In general, the diffusivity decreases from LFSE, to transition elements, to REE, and to HFSE, a trend that can be correlated to the increase of charge in the same order. The activation energy shows a similar trend, increasing from 129 kJ/mol for Rb to 189 kJ/mol for Zr (Table 3, Fig. 6) The transition elements Fe and Cr display the highest activation energies (193 and 228 kJ/mole, respectively) and deviate from this trend.

3.6. Effect of H_2O on Trace Element Diffusion

Trace element diffusion in andesitic melt is significantly enhanced by dissolved water (Fig. 7) Addition of 4.5 wt.% H_2O to anhydrous melt increases the diffusivity of most of the elements, including the LFSE Rb and the HFSE Zr, by one and a half orders of magnitude at 1400°C. This suggests that the effect is mainly related to the viscosity of the melt (see below). Interestingly, the effect of H_2O is much less pronounced for Cr and Eu, which may be explained by a higher proportion of divalent cations in the dry melt than in the hydrous melt for these cations. Oxygen fugacity in the experimental capsule is controlled by the reaction $H_2 + \frac{1}{2}O_2 = H_2O$. Assuming in first approximation a Henrian behavior of water solubility, i.e., concentration of dissolved water being proportional to water fugacity, at (constant) intrinsic hydrogen fugacity imposed by the IHPV, the oxygen fugacity is about two orders of magnitude lower in the nominally anhydrous sample than in the hydrous sample.

4. DISCUSSION

4.1. Systematics of Trace Element Diffusion

Several attempts have been made to develop empirical models for the prediction of diffusion coefficients or the activation

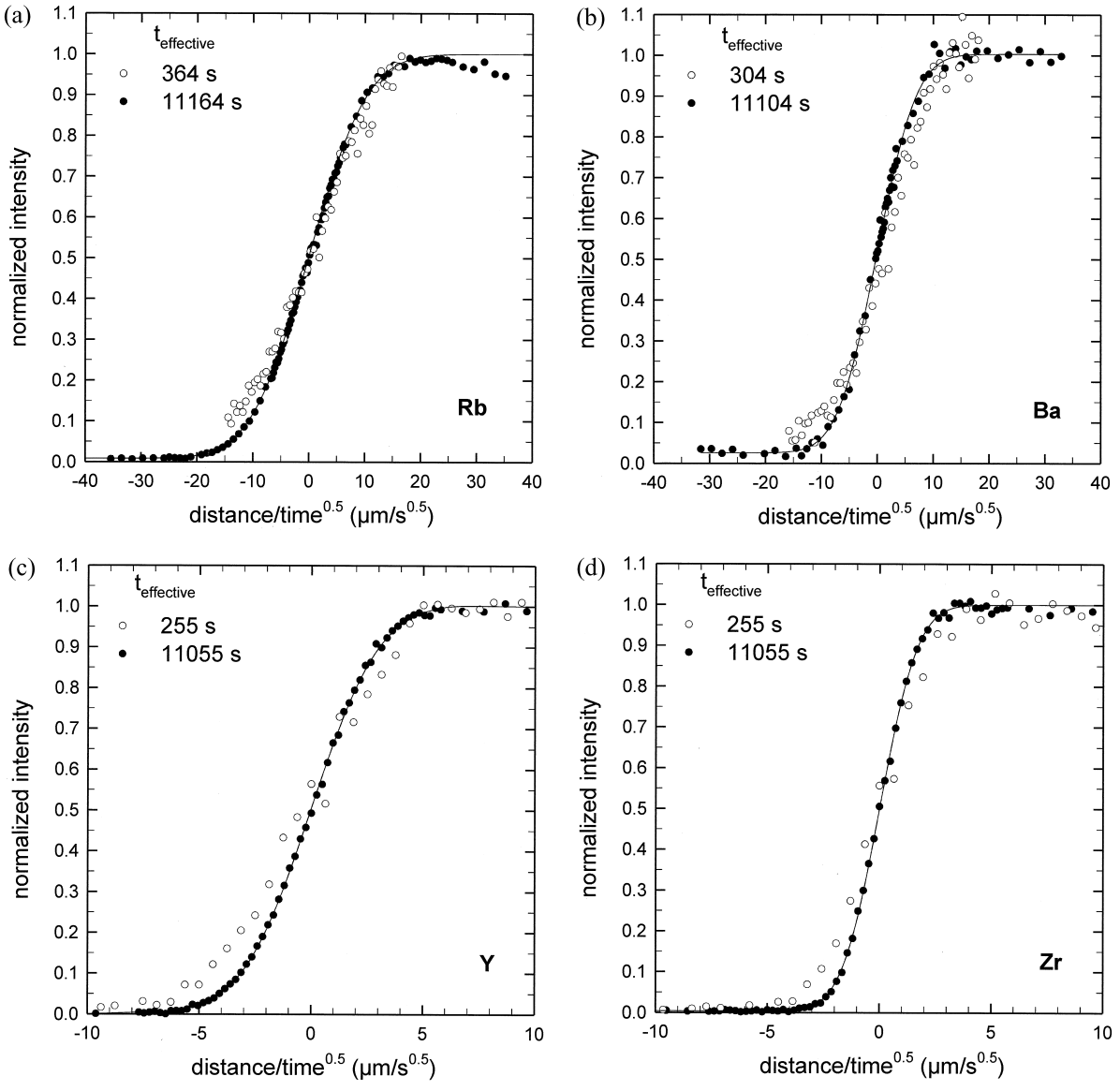

Fig. 3. Trace element diffusion in hydrous andesitic melt at 1100°C and 500 MPa. Maximum intensities are normalized to 1 for comparison. The solid line is a fit for the long term run. Note the good agreement of zero-time and long term run indicating control of transport by diffusion.

energy of diffusion (see reviews of Hofmann, 1980; Jambon, 1982; Watson, 1994; Chakraborty, 1995 and references therein). However, there are no general relationships valid for all elements under all conditions.

A decrease of diffusivity with the charge was demonstrated for diffusing species with similar radius (He, Na^+, Ca^{2+}, Ce^{3+}) in granitic melts (Jambon, 1982). A correlation between activation energy and the squared valence was derived from these data. Corresponding data are not available to test this relationship for other natural melts.

A negative correlation between cation radius and diffusivity is evident for diffusion of alkali and alkaline earth elements in granitic melts below 1000°C (Jambon, 1982). Interestingly, data of Mungall et al. (1999) show an opposite trend for alkaline earth elements in haplogranitic melts at high temperature (1170–1600°C). Our diffusion data for Sr and Ba in andesitic melts are consistent with the trend observed by Jambon.

Several attempts were made to consider combined effects of charge and radius on cation diffusivity. Baker and Watson (1988) observed a poor correlation between diffusivity and ionic field strength defined as z/r (z-cation charge, r-ionic radius) for major and trace element diffusion in compositionally complex Cl- and F-bearing silicate melts. Hofmann (1980) found a linear decrease of log D with z^2r for numerous cations, from monovalent Na to pentavalent V in basaltic melts at 1300°C. However, the comprehensive data sets from Jambon (1982) and this study show that a similar relationship does not apply to granitic and andesitic melts.

To evaluate systematic trends of our diffusion data for hy-

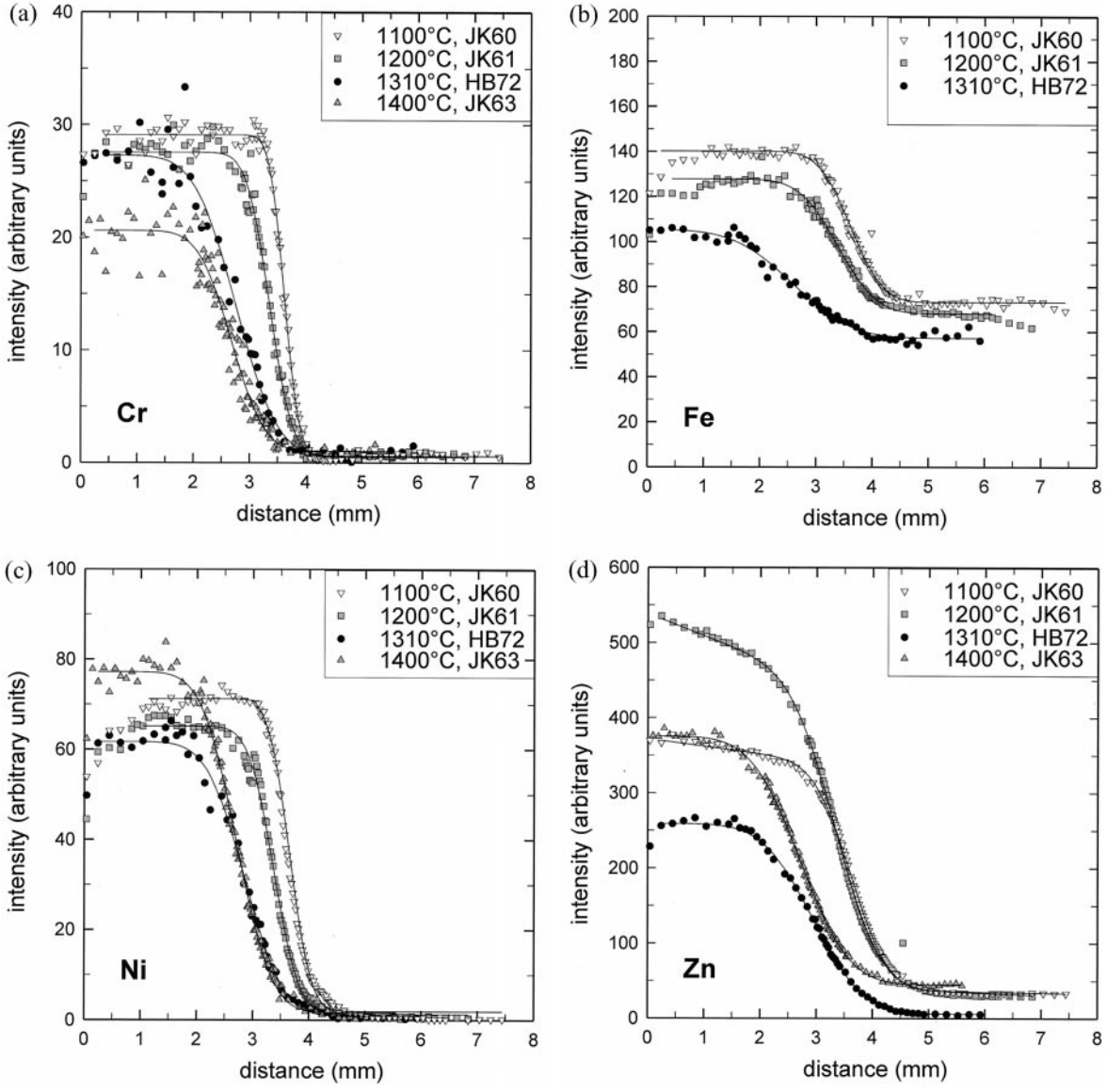

Fig. 4. Trace element diffusion profiles of heterovalent cations in hydrous andesitic melt at 500 MPa. The distance is measured relative to the end of the doped half of the diffusion couple. At 1100 and 1200°C, the Zn concentrations apparently vary with distance in the doped half. This is an artefact of SYXRF measurement observed in some profiles of these particular experiments. To evaluate the profiles a straight line was fitted to the data in the range, which is not affected by diffusion. Dividing measured intensities by the values of the fitted straight line, the profiles excellently are fitted by Eqn. 1.

drous andesitic melts, we have plotted log D as a function of ionic field strength in Figure 8. The ionic field strength is a parameter often used in geochemistry to characterize the behavior of trace elements in geologic processes. In contrast to Baker and Watson (1988), we have used the definition of ionic field strength as the ratio of charge to the squared distance between cations and oxygen (r_{M-O}) proposed by Dietzel (1942). To calculate r_{M-O}, we have used cation ratios and the radius of three coordinated oxygen from Shannon (1976). The assignment of charge and coordination numbers follows Brown et al. (1995) for most of the elements. It should be noted, however, that especially the coordination numbers may depend on melt composition and experimental conditions, and they are not known for the andesitic melt investigated in our study. We assume the large alkali, alkaline earth, and rare earth elements to be 8-coordinated, and the smaller REE (Er, Yb), the transition elements, and the HFSE to be 6-coordinated. Iron and zinc often are 4-coordinated in silicate glasses (see Mysen, 1991; Brown et al., 1995 and references therein), but as we do not know their coordination in our melts, for simplicity we assume them to be 6-coordinated too. A higher coordination number in hydrous melts is supported by recent results of Farges et al. (in press) who show that dissolved water increases the coordination number of nickel from 5 to 6 in sodiumtrisilicate and albite glasses. Most of the elements have a well-known single oxidation state, but some occur in two oxidation states in magmatic systems. Chromium usually is trivalent but may be divalent at very reducing conditions (Schreiber et al., 1978; Keppler,

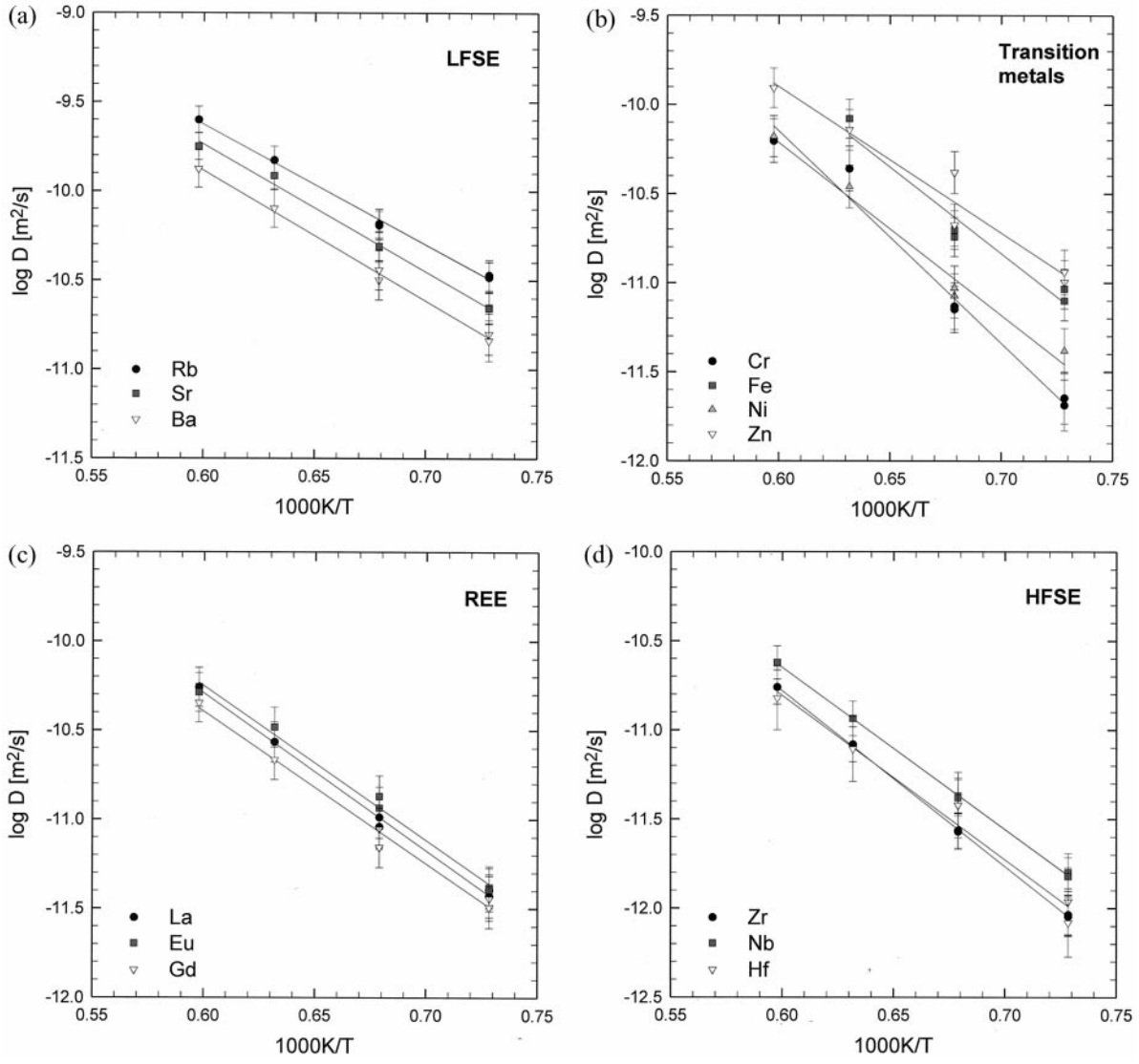

Fig. 5. Arrhenius plot of trace element diffusion in hydrous andesitic melts at 500 MPa.

1992). Iron and europium are both divalent and trivalent under intrinsic conditions of the IHPV (Wilke and Behrens, 1999). On the other hand, the transition elements nickel and zinc have a clear preference for the divalent state in silicate glasses (Brown et al., 1995).

The trace element diffusivity roughly shows a negative correlation to the ionic field strength (Fig. 8). However, there are some systematic deviations from this trend. Sr clearly has a higher diffusivity than Ba (see also Fig. 5a). This is consistent with the trend (increasing diffusivity with decreasing radius) observed for alkalis in granitic melts (Jambon 1982), but opposes the trend for alkaline earth elements in haplogranitic melts (Mungall et al., 1999). Higher diffusivities for Sr compared to Ba were found also in jadeite and in diopside melt at high pressure (Nakamura and Kushiro, 1998). For the andesitic melt, other divalent cations, Zn^{2+} and Ni^{2+}, however, do not follow the trend of alkaline earth elements. These cations show a similar trend observed for REE and HFSE.

Although the REE have constant diffusivity within experimental error, a small but systematic decrease of diffusivity with ionic radius is visible for the trivalent cations at all temperatures. The diffusivity of Y matches the data of the heavy REE very well. The activation energy of Y fits with those of the heavy REE; there is no indication for an anomalous diffusion behavior of Y as reported by Mungall et al. (1999) for a hydrous granite melt. Eu has a higher diffusivity than the neighbor elements Gd and Sm, which can be explained by the contribution of Eu^{2+} to the transport. All other REE are in trivalent state only. The trend of the trivalent REE matches with the data of the HFSE Zr and Hf, and at least at 1100°C, the transition metal Cr. At higher temperature the data of Cr clearly display an offset to the trend of REE and HFSE increasing with temperature. This can be interpreted by an increasing contribution of Cr^{2+} to the transport of chromium, which also explains the relatively high activation energy for Cr diffusion. The activation energy is not only determined by the energy barrier for jumps of the cations, but also by the relative abundance of the diffusing species. An increasing stability of more

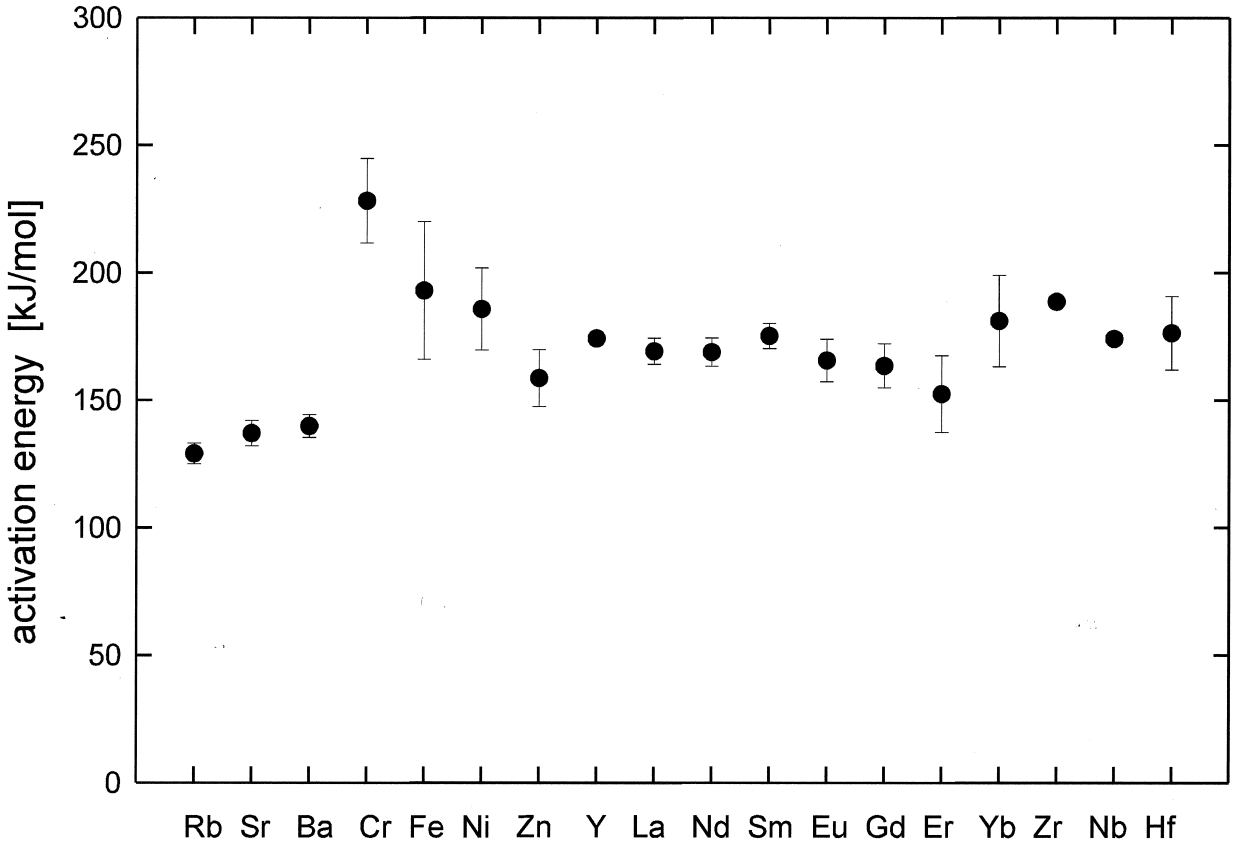

Fig. 6. Activation energy for trace element diffusion in hydrous andesitic melt at 500 MPa.

mobile divalent cations with increasing temperature is expected due to entropic effects. The divalent state is favored over the trivalent state because gaseous O_2, which is formed by reduction, has a much higher entropy than the condensed species. The relatively high activation energy for Fe diffusion can be explained in the same way: by an increasing abundance of divalent iron with increasing temperature.

Another interesting element is niobium, which is usually considered to be Nb^{5+} under magmatic conditions (e.g., Keppler, 1993; Horng et al., 1999). The diffusivity of Nb in the andesitic melt always is higher than that of the 4+ cations Zr and Hf, which have almost identical diffusivity. This is inconsistent with niobium being exclusively Nb^{5+}. A large portion of Nb^{3+} in the melt is required to explain the relative high diffusivity of this element. However, to the authors' knowledge there are no spectroscopic data for an unambiguous assignment of the oxidation state of this element. Other indirect information about the oxidation state of Nb in silicate melts may be derived from experimental partitioning of Nb and Ta between crystals and melts. Although Nb^{5+} and Ta^{5+} show nearly identical geochemical behavior, the ratio of partitioning coefficients, D_{Nb}/D_{Ta}, for some Ti-phases differs significantly from unity (Green and Pearson, 1987; Horng and Hess, 2000). One possible explanation for the difference in the partition coefficients is that Nb partly exists as Nb^{3+} in the silicate melt. However, as shown by Green and Pearson (1987), the partition coefficients are not affected significantly by oxygen fugacities. Therefore, it is unlikely that Nb^{3+} is responsible for the observed partitioning effect. Thus, the reason for the relatively high diffusivities in andesitic melts for Nb compared to Zr melts remains unclear.

An empirical relation that has often been used successfully to predict diffusivities is the so-called *Compensation Law*, suggested by Winchell (1969) and Winchell and Norman (1969). These authors showed that in silicates there is a positive linear correlation between log D_0 and E_a. However, as discussed by Chakraborty (1995), there is no theoretical basis for this relation, and it is only a rough correlation between data, not an exact prediction. Our data for the anhydrous andesitic melt are consistent with this statement (Fig. 9) Although the data show an almost linear trend, the scatter is obvious and deviation from the regression is in part clearly beyond the experimental error.

4.2. Modeling the Diffusivity of Heterovalent Elements

A phenomenologic description of tracer diffusion in one dimension is by Ficks' first law:

$$J_M = -D_M dc_M/dx \quad (4)$$

where J_M is the flux, D_M is the diffusion coefficient, c_M is the concentration of an element M, and x is the distance in direction of diffusion. If M is present in two oxidation states, M^{2+} and M^{3+}, as in the cases of Fe and Eu, the total flux of M is given by:

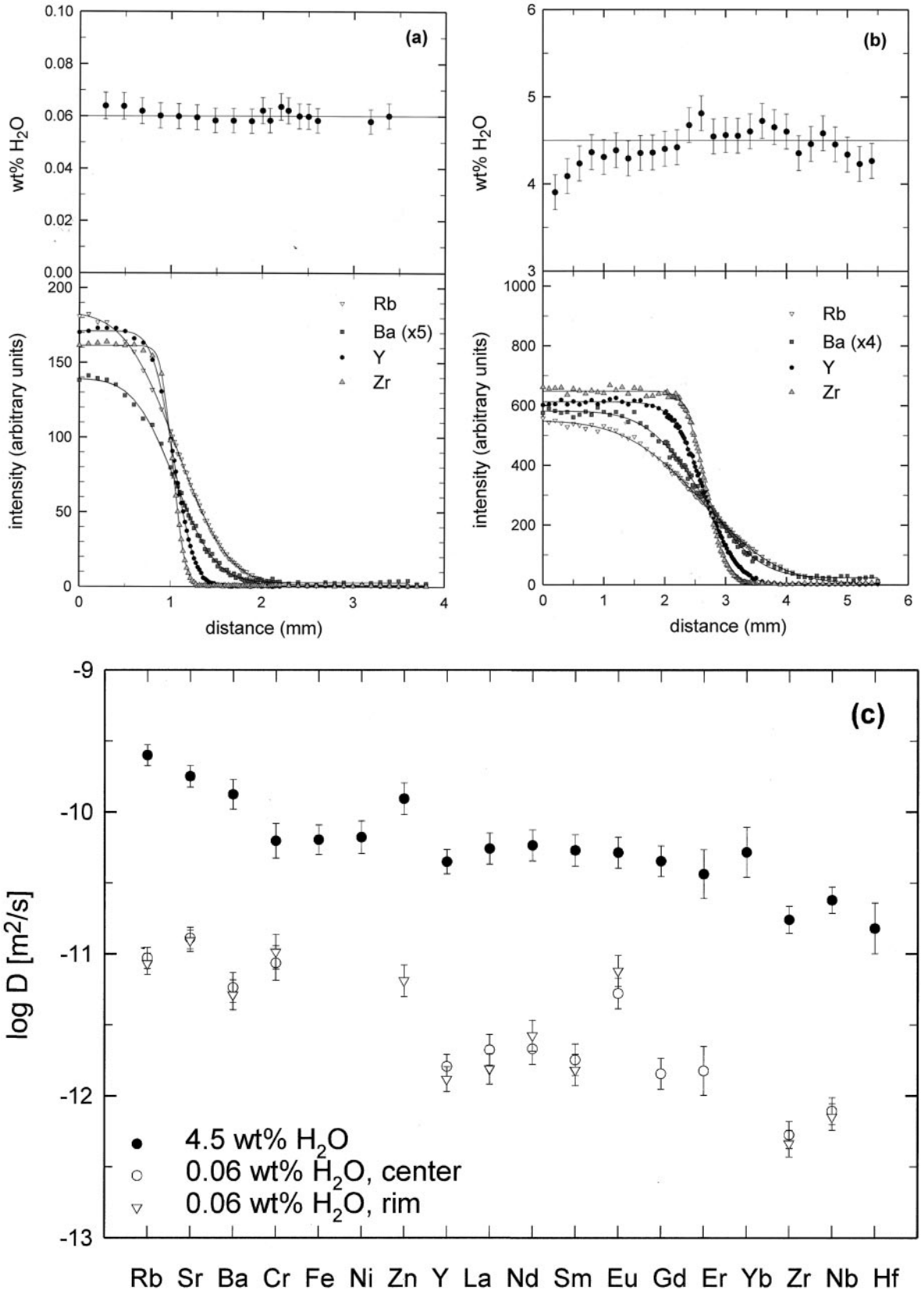

Fig. 7. Comparison of trace element diffusion in anhydrous and hydrous andesitic melts at 1400°C and 500 MPa. (a) Profiles in anhydrous melt measured in the center. (b) Profiles in hydrous melt measured in the center. (c) Comparison of diffusion coefficients.

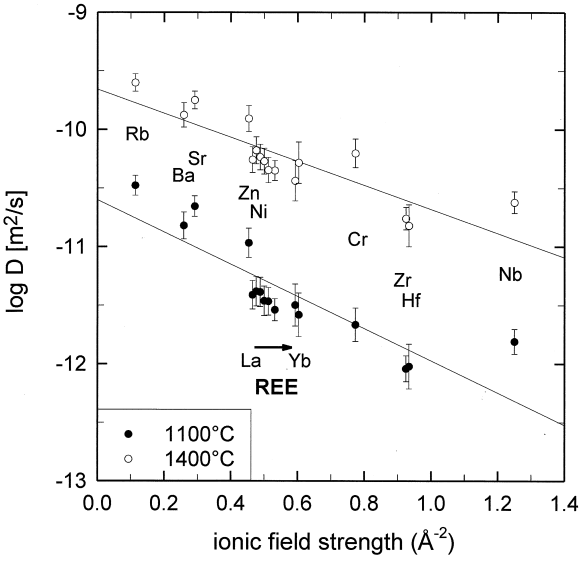

Fig. 8. Correlation between cation diffusivity in hydrous andesitic melts and ionic field strength ($z/r^2_{M\text{-}O}$). Ionic radii are from Shannon (1976). Data at 1100°C are the average of two measures on same sample. Lines are linear regressions of all data for each temperature. Plotted are only elements with clear preference for one oxidation state.

$$J_M = J_{M2+} + J_{M3+} \quad (5)$$

$$J_M = -(D_{M2+}\, dc_{M2+}/dx + D_{M3+}\, dc_{M3+}/dx) \quad (6)$$

Diffusion of multi species component and the role of speciation during diffusion was discussed by Zhang et al. (1991), using oxygen and water transport in silicates as an example. A similar approach may be applied to diffusion of polyvalent elements. Combination of Eqn. 4 and (6) yields:

$$D_M = D_{M2+}\, dc_{M2+}/dc_M + D_{M3+}\, dc_{M3+}/dc_M \quad (7)$$

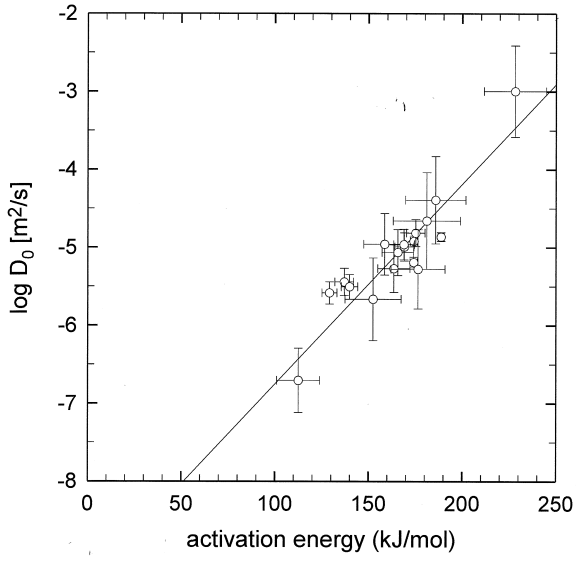

Fig. 9. Compensation law for hydrous andesitic melt.

Table 4. Proportions of divalent Eu estimated from diffusion data.

Run	T (°C)	Profile	Eu^{2+}/Eu_{total}
JK 60, wet	1100	Center, 1	0.03
		Center, 2	0.05
JK 61, wet	1200	Center	0.07
		Rim	0.14
HB 72, wet	1310	Center	0.09
JK 63, wet	1400	Center	0.02
JK 67, dry	1400	Center	0.32
		Rim	0.56

Assuming local equilibrium of reactions among the species (M^{2+} and M^{3+}), and a constant ratio of c_{M2+}/c_M ($=K_2$) at any point in the diffusion zone, Eqn. 7 becomes:

$$D_M = D_{M2+}K_2 + D_{M3+}(1 - K_2) \quad (8)$$

The equation can be rewritten as:

$$K_2 = (D_M - D_{M3+})/(D_{M2+} - D_{M3+}) \quad (9)$$

Knowing D_M, D_{M2+}, and D_{M3+} the ratio of the divalent cations can be calculated from this equation. In general, the uncertainty of diffusion coefficients obtained in individual experiments is too high (>15%) to enable a precise determination of the redox ratio, but data obtained in a single run have a higher relative precision and thus may be suitable to test the method. As an example we have chosen Eu because data are available for Sr^{2+}, which has a similar ionic field strength than Eu^{2+} and for Sm and Gd, which both are in trivalent state, and the average of D_{Sm3+} and D_{Gd3+} is a good estimation of D_{Eu3+}. The calculated ratios Eu^{2+}/Eu_{total} are given in Table 4. At all temperatures, Eu^{3+} clearly dominates in the hydrous melt, whereas in the water-poor melt at 1400°C, the ratio of Eu^{2+}/Eu^{3+} is close to unity. An analog treatment of the other heterovalent elements Cr, Fe, and Nb is not possible due to a lack of reliable estimates of the diffusion coefficients of the cations.

Unfortunately, there are very little experimental data on the effect of redox conditions on diffusion of heterovalent elements in silicate melts. LaTourette and Wasserburg (1997) studied the effect of oxygen fugacity on the diffusion of some elements, including Eu in a haplobasaltic system at 1 atm. Decreasing oxygen fugacity from air to Fe-FeO buffer conditions at 1400°C increased the Eu diffusivity by a factor of two, whereas the Nd diffusivity remained unchanged. Linnen et al. (1996) found a relatively fast diffusion of tin in hydrous haplogranitic melt under reducing conditions where Sn^{2+} is the dominant species, and a relatively low diffusion under oxidizing conditions where Sn^{4+} is dominant (one order of magnitude difference in the diffusion coefficients).

It is noteworthy that a critical point in modeling the diffusion of polyvalent cations is the assumption of local equilibrium of the species. This precondition requires that the time scale of oxidation and reduction of species is short compared to the jump frequency of the species. In the hydrous melt, a rapid oxidation and reduction can be achieved by the reaction:

$$H_2O + MO = H_2 + MO_{1.5} \quad (10)$$

because the diffusion of H_2O and H_2 in water-rich silicate melts is much faster than the diffusion of divalent and trivalent

cations (Chekmir et al., 1985; Behrens and Nowak, 1997). In a dry melt, however, kinetics of redox reactions may be too slow to rapidly achieve local equilibrium. In the extreme situation that species do not change their oxidation state during the experiment, the profile of the polyvalent element is a superimposition of two independent species profiles. In this case a strong deviation of the measured profile from simple error function shape as described by Eqn. 1 is expected, if the diffusion coefficients of the species differ largely. Such a deviation from error function shape was not observed in any of our experiments.

4.3. Comparison to Diffusion Data for Andesitic, Granitic, and Basaltic Melts

Lowry et al. (1982) studied the tracer diffusivity of several elements in an anhydrous andesitic melt at temperatures between 1300 and 1400°C at 1 atm using the radiotracer method. Their diffusion coefficients for Ba and Sr are 0.4 and 0.2 orders of magnitude higher than our data for the water-poor melt at 1400°C (Table 2). Considering the difference in chemical composition, oxygen fugacity, and pressure, the agreement of the diffusion data is very good.

A comprehensive data set for trace element diffusion in haplogranitic melts at dry and hydrous conditions was published recently by Mungall et al. (1999). Although their experiments in the dry system were conducted at ambient pressure, the data may be compared to our results because the effect of pressure on diffusivity usually is small (Watson, 1981; Jambon, 1982). In general, the diffusivity is higher in dry andesitic than in dry haplogranitic melts. However, the effect of composition depends on the geochemical groups. At 1400°C the difference is ~1 log unit for the LFSE Sr and Ba, ~1.5 to 2 log units for the REE Nd and Y, and ~2 to 2.5 log units for the HFSE Zr and Nb. Data from Lesher (1994) at 1 GPa and Perez and Dunn (1996) at 1 atm for Sr and Nd show the same trend, with diffusion in dry granite-like melts at 1400°C being ~0.5 to 1 log units slower than in andesitic melts. As the temperature dependence for viscous flow is much larger for granitic than for andesitic melts (Dingwell et al., 1992; Richet et al., 1996), the deviation increases with decreasing temperature.

In contrast to these trends, data for LFSE diffusion (Rb, Sr, Ba) in natural obsidians (Jambon, 1982; Magaritz and Hofmann, 1978a) extrapolated to 1400°C are similar to data for the dry andesitic system. This inconsistency probably is caused by low but significant water content in the natural obsidians (~0.5 wt.%), because even low concentration of water can strongly accelerate migration of cations in rhyolitic melts (Jambon, 1982).

Baker and Watson (1988) and Baker (1990) extracted trace element diffusion data from experiments on interdiffusion between dry silicic melts differing in bulk composition. These authors demonstrated the similarity of chemical diffusivities of all non-alkali elements, including the trace elements Mn, Zn, Y, Zr, and Nb (Baker and Watson 1988) and Sr, Y, Zr, and Nb (Baker 1990) for interdiffusion between silicic melts (e.g., dacitic and rhyolitic melts in Baker 1990). In general, the diffusivities of all measured trace elements are similar to Si diffusivity. The uniformity in the diffusivities contrasts with the data of Mungall et al. (1999) for a dry haplogranitic melt, and with our data for a dry andesite melt, which are characterized by great differences in the diffusivities of elements from different geochemical groups (see above). This discrepancy can be attributed to the large chemical gradients in the diffusion experiments of Baker and Watson (1988) and Baker (1990).

Diffusion coefficients for dry basaltic melts from Lesher (1994) at 1 GPa for Sr and Nd, from LaTourrette et al. (1996) at 1 atm for Ba, REE, and Zr, from Lowry et al. (1982) for Sr, and Ba, from Hofmann and Magaritz (1977) at 1 atm for Sr and Ba, and from Magaritz and Hofmann (1978b) at 1 atm for REE are generally higher than for andesitic melts at 1400°C. As in the granitic system, the relative deviation in diffusivity depends on the nature of the diffusing species. It is low for the LFSE (~0.5 log unit), medium for the REE (~1 log unit), and relatively high for the HFSE (~1.3 log unit). In summary, as expected from the viscosity behavior, the trace element diffusion coefficients in a dry andesitic melt range between those in dry granitic (high-viscous) and dry basaltic (low-viscous) melts.

Few data only are available for hydrous melts. Diffusion coefficients for hydrous granitic melts (Mungall et al., 1999, 3.7 wt.% water) are generally higher than for hydrous andesitic melt (5 wt.% water). However, the difference in diffusivity between granitic and andesitic melt is smaller for hydrous melts than for dry melts, and it is more or less constant for all elements (at 1300°C 0.7–0.9 log units for hydrous melts compared to 1–2.5 log units for dry melts). The water-induced enhancement of diffusion is much more pronounced for granitic than for andesitic melts. At 1400°C in the granitic system, the diffusion coefficients range increases by 1.8 log units (LFSE) to 2.9 log units (HFSE) if 3.7 wt.% water is added to the nominal dry melt (Mungall et al., 1999). For the less polymerized andesitic melt, the enhancement is, at the same temperature, more or less constant with a mean value of ~1.4 log units when increasing the water content from 0.06 to 5 wt.%.

To the authors knowledge, no trace element diffusion data for hydrous basaltic melts exist. Extrapolating the trends from granitic and andesitic melts to basaltic melts, the mobility of trace elements in a hydrous basaltic melt containing a few percent water is expected to be constantly higher by ~1 log unit than in hydrous andesitic melts at 1300°C, with the difference increasing with decreasing T.

4.4. Comparison with Viscosity Data

With the premise that thermally activated jumps of atoms control diffusion as well as viscous flow, the Eyring model based on absolute reaction theory may be a good approximation to connect transport properties of silicate melts. In fact, choosing a characteristic jump distance λ close to the size of SiO_4 tetrahedra, the Eyring equation:

$$D = k\,T/\lambda\eta \tag{11}$$

(k = Boltzmann constant, η = viscosity) has been used with remarkable success in a variety of melts to relate diffusivity of oxygen or silicon and viscosity (see Chakraborty, 1995).

Viscosities of andesitic melts were computed after Richet et al. (1996) combining their Eqn. 4 and 5 with the unconstrained Vogel-Fulcher-Tammann fit for the anhydrous melt. Assuming

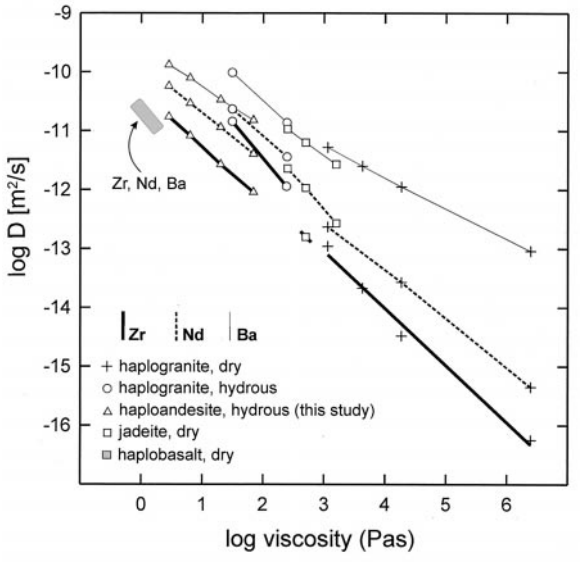

Fig. 10. Variation of trace element diffusion for Zr, Nd, and Ba with viscosity in melts of different compositions. Haplogranite: Mungall et al. (1999); haplobasalt: LaTourrette et al. (1996); jadeite: Nakamura and Kushiro (1998). Line for Zr in dry haplogranite represents a linear regression of the data points. For Zr in the dry jadeite melt, only one data point is available. For the haplobasalt, the data points of Zr, Nd, and Ba plot close together inside the grey field.

Table 5. Quantitative prediction of diffusion coefficients (in m^2/s) for selected elements in a nominal dry andesite melt at 1400°C using linear regression of the hydrous andesite viscosity/diffusivity data.

	Linear regression parameters[a]		log D predicted	log D measured	Relative error (%)
	a	b	1400°C, dry	1400°C, dry	
Rb	−8.69	−0.637	−10.73	−11.05	51.4
Sr	−8.75	−0.669	−10.90	−10.90	0.1
Ba	−8.88	−0.685	−11.08	−11.26	34.6
Y	−9.12	−0.854	−11.86	−11.84	6.1
La	−9.06	−0.835	−11.74	−11.74	0.4
Nd	−9.04	−0.825	−11.69	−11.62	17.1
Sm	−9.03	−0.862	−11.80	−11.78	3.7
Eu	−9.09	−0.797	−11.65	−11.19	187.0
Gd	−9.20	−0.808	−11.79	−11.84	11.1
Er	−9.39	−0.729	−11.73	−11.82	19.4
Zr	−9.42	−0.925	−12.39	−12.31	21.3
Nd	−9.39	−0.853	−12.13	−12.13	0.1

[a] Parameter a and b of the equation $\log D = a + b \log \eta$ (viscosity calculated after Richet et al., 1996 in dPas and diffusion coefficients of the hydrous andesite melts from Table 2 in m^2/s); see Fig. 11 and text for details.

The calculated log viscosities for the hydrous sytstem are 2.84, 2.30, 1.80, and 1.45 dPas for the temperatures 1100, 1200, 1310, and 1400°C, respectively, and 3.21 dPas for the nominal dry melt containing 0.06 wt.% H_2O.

a jump distance of 3 Å, the chemical diffusivity, D_η, calculated by the Eyring relation is in excellent agreement with the tracer diffusivities of the HFSE for both dry and hydrous melt (Table 2). The consistency of the data suggests that the viscosity model of Richet et al. (1996) also is applicable to hydrous andesitic melts in the low-viscosity range; that study measured viscosity of hydrous melts only in the high-viscosity range and combined these data with measurements on anhydrous melts at both low and high viscosity to derive a model applicable in a wide range of temperature and at water contents up to 3.5wt.%. Moreover, because the water content of our hydrous samples is higher than those used in the viscosity study and because the effect of water decreases with increasing water content we infer that the model of Richet et al. (1996) may be applied at even higher water content.

5. APPLICATIONS

5.1. Prediction of Trace Element Diffusivities in Andesitic Melts at Variable Water Contents

In the low-viscosity range, both viscosity and diffusivity often can be described in a good approximation by Arrhenius laws, provided the temperature range is not too large. Thus, plotting log viscosity versus log diffusivity, straight lines are observed with the slope defined by the element specific ratio of the activation energies for diffusion and for viscosity (Fig. 10). The linear D vs. log η relation is an alternate way to show that the Eyring equation works. The correlation indicates that structural relaxation is an important step for migration of cations in the melt. The difference in slope in this plot show that the contribution of structural relaxation to the indivdual jumps of cations through the silicate network depends on the nature of the cation, i.e., its size and charge.

This correlation has interesting perspectives for prediction of trace element diffusivities in andesitic melts with varying water contents as well as for the prediction of diffusivities in other melts, provided viscosity data are available. In turn, viscosities can be estimated from such plots if trace element diffusion data are available.

To test the potential of this approach, for each trace element in hydrous andesitic melts we have calculated the parameter a and b in the equation $\log D = a + b \log \eta$ by linear regressions and then we have used the results to predict trace element diffusivities in the dry melt at 1400°C (Table 5). For most of the trace elements the calculated diffusion coefficients agree within the experimental error with the measured values. Relatively large deviation are observed for the two LFSE Rb and Ba (50 and 30% relative error, respectively) and for Eu (187%). In the case of Eu, the deviation can be explained by different Eu^{2+}/Eu^{3+} ratios in the dry and in the hydrous melts (see Table 4). For the LFSE as well as for other network modifying cations (i.e., Na, K) the log D vs. log η relation probably is not a good tool for prediction of diffusivity because migration of these highly mobile cations is at least partly decoupled from viscous flow.

Although H_2O contents of andesitic melts in nature are poorly constrained, there is evidence from experimental studies on phase equilibria that at least 4 wt.% H_2O must have been dissolved in the melt when amphibole is crystallized (Johnson et al., 1994). At water contents above 2 wt.% the viscosity of andesitic melts only smoothly decreases with water content. Although no experimental data are available, we expect that variation of trace element diffusivity with water content also is small at such high water content. Thus, we infer that application of the log D vs. log η relations based on data for melts

containing ~5 wt.% water can predict the diffusivities for REE, HFSE, and transition metals in natural andesitic melts with an accuracy better than ~50%. However, a prerequisite for reliable predictions is that the melt composition and, in the cases of heterovalent cations, the oxygen fugacity is similar to our experiments. Moreover, for natural iron-bearing andesites it has to be taken into account that the melt viscosity may vary with oxygen fugacity.

Because of the lack of diffusion data for the high-viscous andesite melts it is not clear how far extrapolations of the linear D vs. log η relations to lower temperatures are valid. Since the quality of prediction was successfully tested with the help of a melt with a viscosity of 2.2 Pas, we assume that this method will also predict reliable diffusivities related to viscosities at least up to ~2.5 Pas. These viscosities correspond, for example, to andesite melts with 5 wt.% water at 1000°C, or with 2 wt.% water at 1100°C, respectively, when calculating the viscosities according to Richet et al. (1996). Such conditions are not untypical for andesite magmas (e.g., Johnson et al., 1994).

5.2. Prediction of Trace Element Diffusivities in Other Melts

For a comprehensive trace element modeling of diffusion-controlled magmatic processes, a broad data set of trace element diffusion coefficients for natural-relevant water-bearing melts are needed. If experimental data are not available, diffusivities may be estimated using log D vs. log η relations as outlined above. Fig. 10 shows log D vs. log η relations for selected elements in granitic, andesitic, basaltic, and jadeitic melts. The viscosities were either measured (Mungall et al., 1999, for dry granite; Nakamura and Kushiro, 1998, for dry jadeite) or calculated (this study, using the model of Richet et al., 1996; LaTourrette et al., 1996, using the model of Shaw, 1972, for a dry basalt; Mungall et al., 1999, using the model of Hess and Dingwell, 1996, for hydrous haplogranite). As representatives for the different geochemical groups, Ba (LFSE), Nd (REE), and Zr (HFSE) were chosen. The covered range in diffusion coefficients is large in highly viscous melts and decreases significantly for less viscous melts. In the case of the high-viscous dry granitic melt the diffusivity of Ba is more the three decades higher than Zr (Mungall et al., 1999), whereas in the low-viscous basaltic melt the difference is less than an order of magnitude (LaTourrette et al., 1996). Only the study of Mungall et al. (1999) on dry granitic melts and this study cover a viscosity range wide enough for individually evaluating reliable trends. Both data sets give evidence for linear relations between log D and log η with the slope increasing from Zr to Nd to Ba. Data for dry granitic, dry jadeitic, and hydrous andesitic melts can be described for the three elements with very high precision by single straight lines. However, data for basaltic melts and hydrous granitic melts deviate noticeably from this relationship. At present, it is not possible to clarify whether these deviations really are caused by compositional effects or are due to uncertainties of the experiments or calculations (in the case of viscosity).

5.3. Implications for Modeling Magmatic Processes

The effect of dissolved water on isotope and trace element diffusion in andesitic melts is substantial. After 10,000 yr at 1200°C, diffusion profiles in dry melts are relatively short with lengths (defined as $x = (Dt)^{1/2}$) of 0.8 m for Sr, 0.18 m for Nd, and 0.07 m for the sluggish Zr, representing network forming species (D's calculated from Table 5). In hydrous melts (5 wt.% water) at the same temperature, the profiles are considerably longer: 3.9 m for Sr, 1.9 m for Nd, and 0.92 for Zr (D's from Table 2). The lengthening of the profiles is relatively small for the LFSE (factor ~ 7), medium for the REE (factor ~ 11), and relatively large for the HFSE (factor ~ 14). It is obvious that diffusion can much more effectively decouple isotopic systems like $^{87}Sr/^{86}Sr$ (LFSE) and $^{143}Nd/^{144}Nd$ (REE) in hydrous than in a dry andesitic melts. In dry felsic magma the potential for diffusive decoupling of geochemical systems on a large scale is even smaller. At 1200°C after 10,000 yr, profiles only have lengths of 20 cm for Sr, 2 cm for Nd, and 0.7 cm for Zr (D's from Mungall et al., 1999).

It should be noted that magmatic modeling, which is based only on tracer diffusion data without involving gradients of chemical potentials of components within the melts, is highly idealized because effects of chemical diffusion are ignored. For illustration, Baker (1989) has demonstrated that the chemical diffusivity of Sr during an interdiffusion between dacitic and rhyolitic melts is an order of magnitude lower than the Sr tracer diffusivity in the pure systems. Lesher (1994) proposed an approach using Darken's equation to calculate chemical diffusivity from measured tracer diffusivities. The good agreement between the predicted and the experimentally observed Sr and Nd profiles suggests that this approach has the potential for a realistic modeling of diffusional processes within magmas.

5.4. Europium Anomaly Caused by Diffusive Magma Mixing Processes?

In an experimental study on dry jadeite melt at high pressures, Nakamura and Kushiro (1998) observed diffusion coefficients for Eu being one and a half orders of magnitude higher than for other REE. The authors attributed the relatively fast diffusion of europium to the presence of significant Eu^{2+} due to the relatively low oxygen fugacity in their piston-cylinder apparatus. As a consequence, they concluded that an Eu anomaly can be caused by diffusive mixing of two magmas with different REE concentrations. Our results show only slightly higher diffusivity of Eu compared to its neighbor elements Gd and Sm. Thus, for hydrous andesitic melts, which are commonly regarded as relatively oxidized (NNO to NNO + 3, Johnson et al., 1994), we conclude that a decoupling of Eu from the other REE by diffusion is not very probable.

6. CONCLUSIONS

We have determined the diffusivity of 18 trace elements in a hydrous synthetic iron-free andesitic melt containing 5 wt.% water at a pressure of 500 MPa and at temperatures between 1100 and 1400°C using the diffusion couple technique. The main analytic instrument used in our study was the synchrotron X-ray fluorescence microprobe, which is well suited for the analysis of multi-elemental trace element concentration profiles in silicate systems. The combination of experimental and analytic techniques enables the acquisition of internally consistent sets of trace element diffusion coefficients with a high repro-

ducibility for most of the elements (<15%). For all trace elements, the temperature dependence of diffusion in the hydrous melt can be described by a simple Arrhenius law. In general, the diffusivity decreases from the LFSE to transition elements to REE to the HFSE, a trend which can be correlated to the increase of charge in the same order. The activation energy shows a similar trend increasing from 129 kJ/mol for Rb to 189 kJ/mol for Zr. Due to the breadth and the quality of the data set, it is possible to evaluate small but significant differences between elements of groups of particular geochemical interest, e.g., the diffusion behavior of Fe and Cr (transition elements with varying oxidation state), the diffusivity of Eu or Nb in comparison with the other REE and Zr, respectively. Water has a strong enhancing effect on the trace element diffusivities in andesitic melts. Addition of 4.5 wt.% H_2O to anhydrous melt increases the diffusivity of most of the elements including the LFSE Rb and the HFSE Zr by one and a half orders of magnitude at 1400°C.

Acknowledgments—We thank Otto Diedrich for preparing the delicate samples and Gerald Falkenberg for technical assistance at the SYXRF-microprobe of the HASYLAB, Hamburg. This study was supported by the DFG (BE 1720/6-2) and by the DESY/HASYLAB (I-99-046). This contribution has benefited from critical reviews by J. Mungall, D. Baker, and S. Chakraborty. Valuable editorial advice from C. Romano is acknowledged. We would also like to thank M. Nowak and Y. Zhang for helpful comments.

Associate editor: C. Romano

REFERENCES

Allen C. M. (1991) Local equilibrium of mafic enclaves and granitoids of the Turtle pluton, southeast California: Mineral, chemical, and isotopic evidence. *Am. Mineral.* **76,** 574–588.

Baker D. R. (1989) Tracer versus trace element diffusion: Diffusional decoupling of Sr concentration from Sr isotope composition. *Geochim. Cosmochim. Acta* **53,** 3015–3023.

Baker D. R. (1990) Chemical interdiffusion of dacite and rhyolite: Anhydrous measurements at 1 atm and 10 kbar, application of transition state theory, and diffusion in zoned magma chambers. *Contrib. Mineral. Petrol.* **104,** 407–423.

Baker D. R. (1992) Tracer diffusion of network formers and multicomponent diffusion in dacitic and rhyolitic melts. *Geochim. Cosmochim. Acta* **56,** 617–631.

Baker D. R. and Watson E. B. (1988) Diffusion of major and trace elements in compositionally complex Cl- and F-bearing silicate melts. *J. Non-Cryst. Solids* **102,** 62–70.

Behrens H. (1995) Determination of water solubilities in high-viscosity melts: An experimental study on $NaAlSi_3O_8$ and $KAlSi_3O_8$. *Eur. J. Mineral.* **7,** 905–920.

Behrens H. and Nowak M. (1997) The mechanisms of water diffusion in polymerized silicate melts. *Contrib. Mineral. Petrol.* **126,** 377–385.

Blichert-Toft J., Lesher C. E., and Rosing M. T. (1992) Selectively contaminated magmas of the Tertiary East Greenland macrodike complex. *Contrib. Mineral. Petrol.* **110,** 154–172.

Brown G. E., Farges F., and Calas G. (1995) X-ray scattering and X-ray spectroscopy studies of silicate melts. In *Structure, Dynamics and Properties of Silicate Melts* (ed. J. F. Stebbins, P. F. McMillan, and D. B. Dingwell), *Rev. Mineral.* **32,** 317–410.

Chakraborty S. (1995) Diffusion in silicate melts. In *Structure, Dynamics and Properties of Silicate Melts* (ed. J. F. Stebbins, P. F. McMillan, and D. B. Dingwell), *Rev. Mineral.* **32,** 411–503.

Chekhmir A. S. and Epel'baum M. B. (1991) Diffusion in magmatic melts: New study. In *Physical Chemistry of Magmas* (Advances in Physical Geochemistry, vol. 9; ed. L. L. Perchuk and I. Kushiro), pp. 99–119, Springer-Verlag, New York.

Chekhmir A. S., Persikov E. S., Epel'baum M. B., and Bukhtiyarov P. G. (1985) Hydrogen transport through a model magma. *Geokhimya.* **5,** 594–598.

Chou I. M. (1986) Permeability of precious metals to hydrogen at 2 kbar total pressure and elevated temperatures. *Am. J. Science.* **286,** 638–658.

Dietzel A. (1942) Die Kationenfeldstärken und ihre Beziehungen zu Entglasungsvorgängen, zur Verbindungsbildung und zu den Schmelzpunkten von Silikaten. *Z. Elektrochem.* **48,** 9–23.

Dingwell D. B., Knoche R., Webb S. L., and Pichavant M. (1992) The effect of B_2O_3 on the viscosity of haplogranitic liquids. *Am. Mineral.* **77,** 457–461.

Farges F., Siewert R., Malvergne V., Brown G. E. Jr., Behrens H., and Nowak M. (2000). Transition elements in water-bearing silicate glasses/melts. Part II. Ni in water-bearing glasses. *Geochim. Cosmochim. Acta*, in press.

Gaillard F., Scaillet B., and Pichavant M. (1998) Kinetics of iron oxidation-reduction in hydrous silicic melts. *Terra Nova* **10,** Abstr. Suppl 1, 17.

Green T. H. and Pearson N. J. (1987) An experimental study of Nb and Ta partitioning between Ti-rich minerals and silicate liquids at high pressure and temperature. *Geochim. Cosmochim. Acta* **51,** 55–62.

Grove T. L., Kinzler R. J., Baker M. B., Donelly-Nolan J. M., and Lesher C. E. (1988) Assimilation of granite by basaltic magma at Burnt Lava flow, Medicine Lake volcano, northern California: Decoupling of heat and mass transfer. *Contrib. Mineral. Petrol.* **99,** 320–343.

Haller M. and Knöchel A. (1996) X-ray fluorescence analysis using synchrotron radiation (SYXRF). *J. Trace Microprobe Techniques* **14,** 461–488.

Haller M., Knöchel A., and Radtke M. (1995) New glass capillary optics for the SYXRF microprobe. *Hasylab Ann. Report II* 993–994.

Harrison T. M. and Watson E. B. (1983) Kinetics of zircon dissolution and zirconium diffusion in granitic melts of variable water content. *Contrib. Mineral. Petrol.* **84,** 66–72.

Harrison T. M. and Watson E. B. (1984) The behavior of apatite during crustal anatexis: Equilibrium and kinetic considerations. *Geochim. Cosmochim. Acta* **48,** 1467–1477.

Hess K. U. and Dingwell D. B. (1996) Viscosities of hydrous leucogranitic melts: A non-Arrhenian model. *Am. Mineral.* **81,** 1297–1300.

Hofmann A. W. (1980) Diffusion in natural silicate melts: A critical review. In *Physics of Magmatic Processes* (ed. R. B. Hargraves) pp. 385–417, Princeton University Press, Princeton, New Jersey.

Hofmann A. W. and Magaritz M. (1977) Diffusion of Ca, Sr, Ba, and Co in a basalt melt: Implications for the geochemistry of the mantle. *Jour. Geophys. Res.* **82,** 5432–5440.

Horng W. and Hess P. C. (2000). Partition coefficients of Nb and Ta between rutile and anhydrous haplogranite melts. *Contrib. Mineral. Petrol.* **138,** 176–185.

Horng W., Hess P. C., and Gan H. (1999) The interactions between M^{+5} cations (Nb^{+5}, Ta^{+5}, or P^{+5}) and anhydrous haplogranite melts. *Geochim. Cosmochim. Acta* **63,** 2419–2428.

Jambon A. (1982) Tracer diffusion in granitic melts: Experimental results for Na, K, Rb, Cs, Ca, Sr, Ba, Ce, Eu to 1300°C and a model of calculation. *J. Geophys. Res.* **87,** 10,797–10,810.

Johnson M. C., Anderson A. T., and Rutherford M. J. (1994) Pre-eruptive volatile contents of magmas. In *Volatiles in Magmas* (ed. M. R. Carroll and J. R. Holloway), *Rev. Mineral.* **30,** 281–330.

Kilinc A., Carmichael I. S. E., Rivers M. L., and Sack R. O. (1983) The ferric-ferrous ratio of natural silicate liquids equilibrated in air. *Contrib. Mineral. Petrol.* **83,** 136–140.

Keppler H. (1992) Crystal field spectra and geochemistry of transition metal ions in silicate melts and glasses. *Am. Mineral.* **77,** 62–75.

Keppler H. (1993) Influence of fluorine on the enrichment of high field strength trace elements in granitic rocks. *Contrib. Mineral. Petrol.* **114,** 479–488.

Koepke J., Rocholl A., and Jantos N. (1998) Trace element microanalysis of hydrous silicate melts: The influence of water on SIMS and synchrotron-XRF analysis. *Terra Nova* **10,** Abstract Supplement 1, 31.

Kushiro I. (1976) Changes in viscosity and structure of melt of $NaAlSi_2O_6$ composition at high pressures. *J. Geophys. Res.* **81,** 6347–6350.

Lange R. A. (1994) The effect of H_2O, CO_2, and F on the density and viscosity of silicate melts. In *Volatiles in Magmas* (ed. M. R. Carroll and J. R. Holloway), *Rev. Mineral.* **30,** 331–369.

LaTourette T. and Wasserburg G. J. (1997) Self diffusion of europium, neodymium, thorium, and uranium in haplobasaltic melt: The effect of oxygen fugacity and the relationship to melt structure. *Geochim. Cosmochim. Acta* **61,** 755–764.

LaTourette T., Wasserburg G. J., and Fahey A. J. (1996) Self diffusion of Mg, Ca, Ba, Nd, Yb, Ti, Zr, and U in haplobasaltic melt. *Geochim. Cosmochim. Acta* **60,** 1329–1340.

Lesher C. E. (1990) Decoupling of chemical and isotopic exchange during magma mixing. *Nature* **344,** 235–237.

Lesher C. E. (1994) Kinetics of Sr and Nd exchange in silicate liquids: Theory, experiments, and applications to uphill diffusion, isotopic equilibration, and irreversible mixing of magmas. *J. Geophys. Res.* **99,** 9585–9604.

Linnen R. L., Pichavant M., and Holtz F. (1996) The combined effects of f_{O2} and melt composition on SnO_2 solubility and tin diffusivity in haplogranitic melts. *Geochim. Cosmochim. Acta* **60,** 4965–4976.

Lowry R. K., Henderson P., and Nolan J. (1982) Tracer diffusion of some alkali, alkaline-earth and transition element ions in a basaltic and an andesitic melt, and the implications concerning melt structure. *Contrib. Mineral. Petrol.* **80,** 254–261.

Magaritz M. and Hofmann A. W. (1978a) Diffusion of Sr, Ba, and Na in obsidian. *Geochim. Cosmochim. Acta* **42,** 595–605.

Magaritz M. and Hofmann A. W. (1978b) Diffusion of Eu and Gd in basalt and obsidian. *Geochim. Cosmochim. Acta* **42,** 847–858.

Mungall J. E. and Dingwell D. B. (1997) Actinide diffusion in a haplogranitic melt: Effects of temperature, water content, and pressure. *Geochim. Cosmochim. Acta* **61,** 2237–2246.

Mungall J. E., Romano C., and Dingwell D. B. (1998) Multicomponent diffusion in the molten system K_2O-Na_2O-Al_2O_3-SiO_2-H_2O. *Am. Mineral.* **83,** 685–699.

Mungall J. E., Dingwell D. B., and Chaussidon M. (1999) Chemical diffusivities of 18 trace elements in granitoid melts. *Geochim. Cosmochim. Acta* **63,** 2599–2610.

Mysen B. (1991) Relations between structure, redox equilibria or iron, and properties of magmatic liquids. *Adv. Physical Chem.* **9,** 41–98.

Nakamura E. and Kushiro I. (1998) Trace element diffusion in jadeite and diopside melts at high pressures and its geochemical implication. *Geochim. Cosmochim. Acta* **62,** 3151–3160.

Nowak M. and Behrens H. (1997) An experimental investigation on diffusion of water in haplogranitic melts. *Contrib. Mineral. Petrol.* **126,** 365–376.

Perez W. A. and Dunn T. (1996) Diffusivity of strontium, neodymium, and lead in natural rhyolite melt at 1.0 GPa. *Geochim. Cosmochim. Acta* **60,** 1387–1397.

Pouchou J. L. and Pichoir F. (1991) Quantitative analysis of homogeneous or stratified microvolumes applying the model "PAP." In *Electron Probe Quantification* (ed. K. F. J. Heinrich and D. E. Newbury), pp. 31–75, Plenum Press, New York.

Rapp R. P. and Watson E. B. (1986) Monazite solubility and dissolution kinetics: Implications for the thorium and light rare earth chemistry of felsic magmas. *Contrib. Mineral. Petrol.* **94,** 304–316.

Richet P., Lejeune A., Holtz F., and Roux J. (1996) Water and the viscosity of andesite melts. *Chem. Geol.* **128,** 185–197.

Rossano S., Ramos A. Y., and Delaye J. M. (2000). Environment of ferrous iron in $CaFeSi_2O_6$ glass; contribution of EXAFS and molecular dynamics. *J. Non-Cryst. Solids* **273,** 48–52.

Schmidt B. C. (1996) Conditions de fusion partielle et mecanismes díncorporation de H_2 et H_2O dans les magmas haplogranitiques. Ph.D. thesis, University of Orleans, France.

Schreiber H. D., Thanyasari T., Lach J. J., and Legere, R. A. (1978) Redox equilibria of Ti, Cr, Eu in silicate melts: Reduction potentials and mutual interactions. *Phys. Chem. Glasses* **9,** 126–139.

Schulze F., Behrens H., Holtz F., Roux J., and Johannes W. (1996) The influence of H_2O on the viscosity of a haplogranitic melt. *Am. Miner.* **81,** 1155–1165.

Shannon R. D. (1976) Revised effective ionic radii and systematic studies of interatomic distances in halides and chalcogenides. *Acta Crystallogr. A* **32,** 751–767.

Shaw H. R. (1972) Viscosities of magmatic silicate liquids: An empirical method of prediction. *Am. Jour. Sci.* **272,** 870–893.

Smith J. V. and Rivers M. L. (1995) Synchrotron X-ray microanalysis. In *Microprobe Techniques in the Earth Sciences* (ed. P. J. Potts, J. F. W. Bowles, S. J. B. Reed, and M. R. Cave), pp. 163–233, Chapman & Hall, London.

Snyder D. and Tait S. (1998) The imprint of basalt on the geochemistry of silicic magmas. *Earth Planet. Sci. Lett.* **160,** 433–445.

Tamic N., Behrens H., and Holtz F. (2000). The solubility of H_2O and CO_2 in rhyolitic melts in equilibrium with a mixed CO_2-H_2O fluid phase. *Chem. Geol.*, in press.

Van Espen P. J., Nullens H., and Adams F. (1977) A computer analysis of X-ray fluorescence spectra. *Nucl. Instr. Meth.* **142,** 269–273.

Watson E. B. (1981) Diffusion in magmas at depth in the earth: The effects of pressure and dissolved H_2O. *Earth Planet. Sci. Lett.* **52,** 291–301.

Watson E. B. (1994) Diffusion in volatile-bearing magmas. In *Volatiles in Magmas* (ed. M. R. Carroll and J. R. Holloway), *Rev. Mineral.* **30,** 371–411.

White B. S. and Montana A. (1990) The effect of H_2O and CO_2 on the viscosity of sanidine liquid at high pressures. *Jour. Geophys. Res.* **95,** 15683–15693.

Wilke M. and Behrens H. (1999) The dependence of the partitioning of iron and europium between plagioclase and hydrous tonalitic melt on oxygen fugacity. *Contrib. Mineral. Petrol.* **137,** 102–114.

Winchell P. (1969) The compensation law for diffusion in silicates. *High Temp. Science* **1,** 200–215.

Winchell P. and Norman J. H. (1969) A study of the diffusion of radioactive nuclides in molten silicates at high temperatures. In *Third International Symposium on High-Temperature-Technology Proc.* pp. 479–492, Butterworth, London.

Zhang Y. (1999) H_2O in rhyolitic glasses and melts: Measurement, speciation, solubility, and diffusion. *Rev. Geophys.* **37,** 493–516.

Zhang Y. and Stolper E. M. (1991) Water diffusion in basaltic melts. *Nature* **351,** 306–309.

Zhang Y. and Behrens H. (2000) H_2O diffusion in rhyolitc melts and glasses. *Chem. Geol.* **169,** 243–262.

Zhang Y., Stolper E. M., and Wasserburg G. J. (1991) Diffusion of a multi-species component and its role in oxygen and water transport in silicates. *Earth Planet. Sci. Lett.* **103,** 228–240.